

# Graphene-metal oxide nanocomposites for supercapacitors: A perspective review

Vardhaman V. Khedekar, Shaikh Mohammed Zaeem and Santanu Das\*

*Department of Ceramic Engineering, Indian Institute of Technology (BHU), Varanasi, UP, India 221005*

DOI: 10.5185/amlett.2018.1932

[www.vbripress.com/aml](http://www.vbripress.com/aml)

## Abstract

Graphene-Metal oxide nanocomposites have been extensively investigated due to their potential applications in the fields of energy devices, including, solar cells, fuel cells, batteries, sensors, electro-catalysis, and photo-catalysis. Among them, several researches have been performed on supercapacitors, which could be best used with devices that require high current for short duration of time. Here, in this article, we present a brief review on the recent advances on the graphene-metal oxide nanocomposites for supercapacitor technologies and the future perspective of this field of research. A wide range of graphene-metal oxide synthesis techniques have been discussed with a focus on the advancement of nanocomposites with controlled features, including, particle size, morphologies, surface structures, pore size, pore-distributions, etc. Specifically, various nanocomposites and their role in supercapacitor electrodes are discussed with their explicit electrochemical charge-storage mechanisms along with charge-transfer techniques. Furthermore, this analysis demonstrates current trends and future directions in research on graphene-metal oxide nanocomposite electrodes for the performance enhancement in next-generation supercapacitor devices. Copyright © 2018 VBRI Press.

**Keywords:** Graphene, metal oxides, nanocomposites, electrocatalytic electrodes, supercapacitor.

## Introduction

Sustainable clean energy demand is currently deliberated as one of the most alarming global issues in the near time owing to the huge energy consumption associated with extensive carbon di-oxide (CO<sub>2</sub>) emission, which could seriously affect the human survival. Specifically, the renewable energy resources became consistently important due to the accelerated growth of global economy with inflated world population, climate change, and decreasing resources of fossil fuels. Recently, World Energy Scenarios 2016 report shows that per capita global energy demand will increase before 2030 and the increasing demand will reach double to its present energy supply by 2050 ([www.worldenergy.org](http://www.worldenergy.org)). Furthermore, the rapid increase in human dependency on energy-consuming devices and abundant use of electronic devices results in the growing need for developing new types of clean energy conversion and storage systems, including, solar cells, supercapacitors, batteries, and fuel cells, which are ultra-low exhaust emission systems. Presently, lithium-ion batteries (LIB) are the prevalent energy storage unit for the portable electronics due to their good energy density. However, the capabilities of LIBs are put down by the modern multifunctional portable electronic devices because of the progressive demand of an energy storage device with high power density. In this regard, supercapacitors, which are currently emerging as a promising alternative energy storage technology, are considered as one of the strong candidates for accomplishing those requirements where LIBs are unable to fulfil existing demands. This is affirmed by the fact that

the world market of supercapacitors has been growing increasingly and will worth \$86 billion by 2023. Compared to LIBs, supercapacitors exhibit ultra-high energy density and power density, ultra-fast charge discharge rate, lightweight, and do not depend on any complex chemical action to store energy, thus, they have long life-cycles compared to LIBs. In addition, due to simple architecture, supercapacitor can be configured into a flexible energy storage device, which is an added advantage of the system to be useful for their future applications in flexible electronic devices.

Supercapacitors, are also known as "electrochemical capacitors" or ultra-capacitors, are one of the major electrochemical energy storage devices having capability of storing electrical energy at much higher amount and rate than that of the conventional capacitors and batteries. Owing to their relatively higher specific power density and low internal resistance, supercapacitors are able to store and deliver energy at relatively higher rates as compared to other energy storage devices.

The typical supercapacitor device consists of two identical electrodes, electrolyte medium, and a porous membrane called separator as shown in **Fig. 1**, which demonstrate the electrolyte is sandwiched between two identical electrodes with a porous separator that isolates the two electrodes electrically. The electrolyte attributed to an ion-conducting substance, which can be a diluted acid solution, salt solution, solution of organic material or an ionic liquid. In a typical supercapacitor, the energy storage (i.e. charging of a supercapacitor) mechanism involves a simple charge separation at the interface

between the electrode and the electrolyte and the discharge mechanism involves the process of combination of separated charges in electrolyte while the device delivers the stored energy into an external load. Also, in a supercapacitor device, electrodes (i.e. cathode and anode) are very important components, which play a pivotal role in catalytic charge-transfer at the interface between electrode and electrolyte, thus, electrode materials primarily contribute to the capacitance, power density, energy density, and charge-discharge rates of a supercapacitor. "Capacitance" deals with the charge-storage capacity of a supercapacitor device according to their active electrode materials and can be categorized into three different categories, including, gravimetric capacitance (can be represented as  $Fg^{-1}$ ), areal capacitance ( $Fcm^{-2}$ ), and volumetric capacitance ( $Fcm^{-3}$ ). "Energy density" and "power density" refers to the "capability of energy storage" and "capability of rate of energy transfer to the external devices", respectively. The "energy density", of a supercapacitor can be represented as  $Whkg^{-1}$  (watt hour per kilogram) or  $Whl^{-1}$  (watt hour per liter); while "power density" can be represented as  $Wkg^{-1}$  (watt per kilogram, i.e. gravimetric unit) or  $Wl^{-1}$  (watt per liter, i.e. volumetric unit). All these performance indices are affected by the nature of the electrode material, the nature of electrolyte and the construction of the supercapacitor.

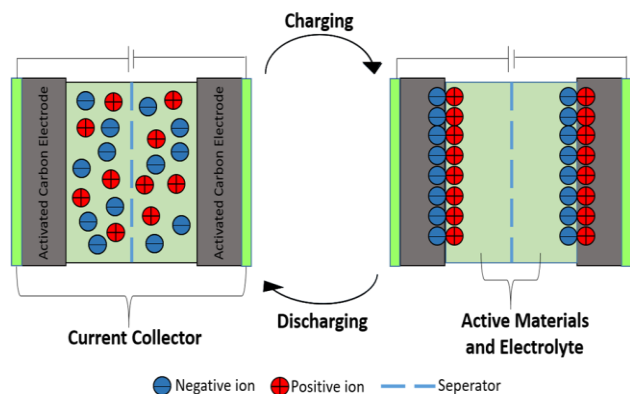


**Fig. 1.** Schematic showing the construction of a typical electric double layer supercapacitor devices in (a) discharged state and (b) charged state.

Carbonaceous or porous carbonaceous materials, which show high electrocatalytic activity, are commonly used as supercapacitor electrode materials which work on the principle of charge storage by electrostatic separation. However, various other electrocatalytic materials like metal oxides ( $MnO_2$ ,  $NiO$ ,  $RuO_2$  etc.) and conducting polymers (polyaniline, polypyrrole etc.) have already demonstrated for their use as supercapacitor electrodes. Especially, metal oxides involve storage based on the faradaic charge transfer. Thus, the nature of electrode material determines the charge storage mechanism and hence based on the charge storage mechanism and the nature of electrode materials, supercapacitors can be classified be into various types as shown in the **Fig. 2**.

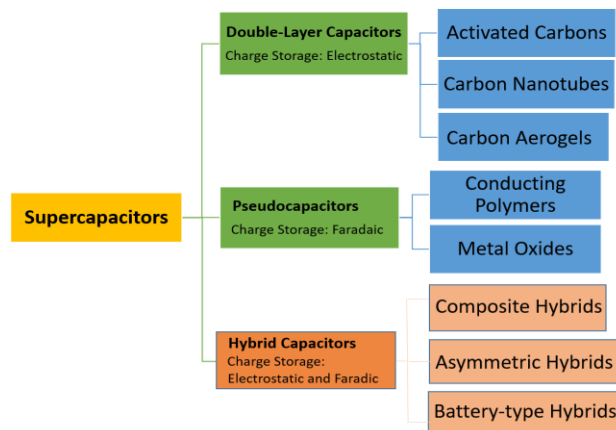


**Fig. 2.** Schematic representation of different types of supercapacitors.

Apart from the choice of materials, application of nanotechnology has created enormous possibilities for the enhancement of supercapacitor performances by applying various nanomaterials, nanostructures, nano-architectures and nano-hybrids as electrode materials. Carbon nanomaterials and their various hybrid architectures have showed huge promise and have been extensively used for high-performance supercapacitor electrodes. These carbon nanomaterials include single walled carbon nanotube (SWNT), fullerene, multi-walled carbon nanotubes (MWNT), activated carbon, graphene, graphene oxide, reduced graphene oxide (rGO), and their hybrid architectures with polymers, metals, metal-organic frameworks(MOFs), and metal oxides.

Graphene, a recently discovered two dimensional,  $sp^2$  bonded single-graphitic layered carbon allotrope, has created unprecedented research interests owing to its very good electrical and thermal conductivity, high surface area ( $2630\text{ m}^2g^{-1}$ ), superior charge-transfer properties, ultra-high mechanical strength, and excellent electrochemical activity. Since its invention, graphene has been extensively used for various electronics [1, 2], optoelectronics[3–5] and electrochemical devices[6–8]. In particular, graphene showed enormous promises for enhancing the performance of various electrochemical devices, including, batteries, supercapacitors, fuel cells, photovoltaics, photo-catalysis, hydrogen generations, water-splitting, sensors, and many more [6, 9, 10]. In graphene, a combination of  $s$ ,  $p_x$  and  $p_y$  orbitals of carbon atoms constitute the in-plane sigma bonds with its neighboring carbon atoms and known as  $sp^2$  hybridized material. The final  $p_z$  orbital electron, which contributes to the pi-bond in graphite, however, leads to the delocalization of electrons for single-layer graphene. The delocalized electrons deteriorate the electrocatalytic activity of graphene, thus, graphene basal-planes are electrocatalytically inert compared to its edge-plane like structures [6, 10]. And to improve the edge-plane like electro-catalytic surface of graphene for faster electron transfer in electrochemical processes, it may require functionalization or development of hybrid architectures. In this regard, graphene nanohybrid materials, have opened up diverse new frontiers by offering new concepts

of novel nanoarchitectures, performance enhancement, and improvements in the reliability of the supercapacitor devices.

The aim of this article is to summarize the recent progress in the field of supercapacitor electrode materials based on synergistically developed graphene-metal oxide nanocomposite materials. In this review, we focus on the various nano-architectures of graphene and different metal oxides and their performances as electrocatalytic electrodes for super capacitor devices. It aims to offer a review of methods of synthesis of graphene, charge storage mechanism in graphene nanohybrids based supercapacitors, followed by systematic discussion on the strategies of improvement (synthesis techniques, structure function relationship etc.) of the electrochemical performance of the hybrid supercapacitor for each graphene-metal oxide. In addition, future perspective of these materials in order to further the improvement in this field of research is also discussed in this report.

### Synthesis of Graphene

Since 2004, graphene has created a huge research interests owing its outstanding electrical, mechanical, thermal and electrochemical properties, which further make graphene viable for commercial and strategic applications for electronics and energy devices. To date, several scientific research and patents have been published on large-scale production of high quality graphene at low cost [1,11]. Graphene synthesis can be categorically classified as bottom-up approaches (e.g., CVD, epitaxial growth on SiC, arc discharge, etc.) and top-down approaches (e.g., exfoliation methods, chemical synthesis) [12, 13]. However, the scalable synthesis of high quality graphene, graphene production on arbitrary substrates, and directional growth of graphene are the key challenges for their utilizations in high-performance next generation energy-devices, such as, supercapacitors.

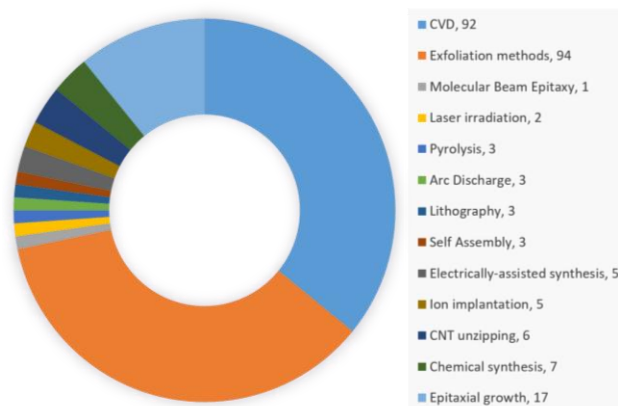


**Fig. 3.** Segmentation of patents filed for various graphene synthesis methods. [Reproduced with permission from ref. [13]].

**Fig. 3** shows the pie chart demonstrating number of publications on various graphene synthesis techniques that have been reported till date. It is quite evident from

**Fig. 3** that substantial number of patents have been disclosed particularly on exfoliation (94 patents) and CVD method (92 patents). However, other synthesis techniques were also published and patented based on epitaxial growth on SiC substrates, chemical synthesis, and unzipping of carbon nanotubes etc. In the following sections, brief overview of some graphene synthesis methods is elaborated. In this review, we are focusing particularly on those graphene synthesis methods, which are relevant for supercapacitor applications.

### Chemical exfoliation

This method directly exfoliates the graphite from graphite flakes in surfactant molecules or organic solvents with the help of ultrasonication [14]. Viculis *et. al* first reported chemically exfoliated few-layer graphite using potassium (K) as an intercalating material [15]. Another important development in this area is the advent of rod-coating (Meyer rod-coating) technique [11] for the industrial-scale production of reduced-graphene oxide-based (rGO) flexible transparent conducting films for touch screen applications. This novel strategy follows a solution-processing approach that combines the rod-coating technique with a newly developed room temperature reduction method [13] to fabricate a large-scale and uniform rGO film directly on PET and Si substrates. These processes are scalable and has capability of depositing graphene on a wide variety of substrates, which is not possible using processes like cleavage or thermal deposition. Also, this method can be used to produce graphene-based composites and films transistors, transparent conductive electrodes, and so on.

### Solution-phase exfoliation

Liquid-phase exfoliation of graphite is based on exposing the materials to a solvent with a surface tension that favors an increase in the total area of graphite crystallites [16]. The solvent is typically non-aqueous, but aqueous solutions with surfactant can also be used. With the aid of sonication, graphite splits into individual platelets, and prolonged treatment yields a significant fraction of mono layer flakes in the suspension, which can be further enriched by centrifugation. It is a direct, simple and low-cost method and is feasible for large-scale production. On the other hand, it is time-consuming and has impure products.

### Chemical Method: Synthesis of graphene oxide and reduced graphene oxide

Chemical method of graphene synthesis is one of the most popular and widely used methods for the production of large scale synthesis of graphene oxide (GO) and reduced graphene oxide (rGO). To date, GO or rGO are the main source of graphene in most of the graphene derived materials in functionalized graphene, graphene-metal oxide nanocomposites, which have been prepared via these chemical routes. Primarily, Hummers method [17], modified Hummers method [18,19], and improved

method [20] are the only available methods for the synthesizing graphite oxide followed by graphene oxide. In this process, graphite powder is mixed with some strong oxidizing agents, like, sulfuric acid ( $\text{H}_2\text{SO}_4$ ), potassium permanganate ( $\text{KMnO}_4$ ), orthophosphoric acid ( $\text{H}_3\text{PO}_4$ ), sodium nitrate ( $\text{NaNO}_3$ ) and graphite was allowed to be oxidized (temperature  $\sim 50$ - $55$  °C) for an extended period of time followed by the neutralization of the acid by hydrogen peroxide ( $\text{H}_2\text{O}_2$ ) as described in detail in elsewhere [12, 21]. Furthermore, the dark brown colored precipitate of graphite oxide is separated out from the solution mixture, washed and vacuum dried, followed by the solution dispersion via sonication in order to produce single layered graphene oxide. The as-produced graphene oxide is reduced back to its original state using various reducing agents and the final product is known as reduced graphene oxide (rGO). Generally, hydrazine hydride [19] is used as one of the strong reducing agent for GO reduction, however other reducing agents like  $\text{NaBH}_4$  and mixture of  $\text{NaBH}_4$  and  $\text{CaCl}_2$  [22] have been used for reducing graphene oxide. In addition, high-temperature thermal reduction methods have been used extensively for producing rGO.

### Chemical vapor deposition

Chemical vapor deposition (CVD) method has an advantage of producing graphene on large-scale by continuous production process. Also, the process is capable of producing large area monolayer graphene or atomically thin few layer graphene films with ultra-high purity, large domain size, and uniform thickness, which has potential applications in next generation miniaturized, lightweight, high-performance and ultra-high capacity energy storage devices, like supercapacitors [13].

In thermal CVD process, graphene is grown directly on a transition metal surface via deposition of carbon, which is produced due to the reduction of hydrocarbon gas at a high temperature under controlled atmosphere [11]. Typically, nickel (Ni) or copper (Cu) foils are used as substrates for graphene growth, however, in some cases, thin-film of Cu and Ni on any substrate is also used as substrate for graphene growth. In particular, for graphene with 3D architecture (*for supercapacitor applications, as discussed in section 3.2.4*), Ni-foams and Cu-forms with varying pore size/pore diameter are used as substrate for graphene growth. In general, for graphene growth in thermal CVD process, methane ( $\text{CH}_4$ ), hydrogen ( $\text{H}_2$ ), and argon (Ar) are used as the precursor gas, reducing gas, and carrier gas, respectively. The reaction temperature for graphene growth in CVD process is performed at  $1000^\circ\text{C}$ , however, several reports of low temperature CVD process is also found that demonstrated the production of graphene at around  $700$ - $900^\circ\text{C}$ . Cooling rate during the CVD process plays an important role in growing graphene on metal substrates, where degree of solubility of carbon in various metal substrate is important in the formation of either uniform monolayer graphene or patchy multilayer graphene sheets on the substrate [12, 23]. However, it is difficult to control the

graphene thickness by controlling number of layer of graphene on any metal surfaces in a thermal CVD process. Despite of various other drawbacks the graphene synthesized in CVD process has attracted considerable importance owing to its scalable synthesis and capability of producing graphene with less structural and electronic disorders [24]. In addition to the synthesis methods discussed above, some other graphene synthesis techniques are equally popular, however, those techniques may not be applicable for supercapacitor applications. Those graphene synthesis techniques are mechanical exfoliation, arc discharge method, epitaxial growth, unzipping of nanotubes etc.

## Charge storage in graphene-metal oxide supercapacitors

### Mechanisms of charge storage in graphene-metal oxide hybrids

In graphene-metal oxide nanohybrids, the total capacitance is a function of charge storage contribution by two processes - electrostatic surface charge storage in graphene, and faradaic charge transfer in metal oxide [25]. The different charge storage mechanism and some key findings on the nature of charge storage is discussed below.

### Electric double layer capacitance

Graphene like other carbonaceous materials involves charge storage based on the separation of charges upon the application of potential at the electrode-electrolyte interface. This is known as Electric Double layer capacitance or non-faradaic capacitive charge storage [26, 27]. They can be said to behave like classical capacitors and therefore, capacitance for a given electrode/ion interface can be given as [28]-

$$C = \frac{A\varepsilon_r\varepsilon_0}{d} \quad (1)$$

where,  $\varepsilon_r$  is the electrolyte relative permittivity,  $\varepsilon_0$  is the vacuum permittivity,  $d$  is the effective thickness of the double layer, and  $A$  is the electrode surface area. Thus, charging occurs when the potential differences are created between two electrodes by accumulating equal and opposite ionic charges on each electrode as shown in **Fig. 1**. However, the positive and negative charges start diffusing into each other when they are discharged. This charge/discharge mechanism inside a EDLC is shown in **Fig. 1**. A capacitive electrode shows linear dependence of the charge stored with changing potential [29]. The ability of any capacitor to store charge is expressed as a differential capacitance given by:

$$C = \frac{dQ}{dV} \quad (2)$$

where,  $dQ$  is the charge stored (expressed in coulombs, C, or mAh) and  $dV$  is the width of the voltage window (V).

Integrating this equation, we can obtain an expression for the energy ( $E$ ) stored within a capacitor, given as-

$$E = \frac{1}{2} CV^2 \quad (3)$$

### Faradaic charge storage

Faradaic charge processes are found in the materials like metal oxides (for example,  $\text{MnO}_2$ ,  $\text{RuO}_2$ ,  $\text{NiO}$ ,  $\text{Co}_3\text{O}_4$  etc.) and conducting polymers (polypyrrole, polyaniline, etc.) which involve surface redox reactions. Here, electron transfer occurs between electrode material and electrolyte i.e. chemical changes occur in the solid phase of the electrode material during the charge-discharge cycle [29]. For the metal oxides, faradaic charge transfer can be classified in three different types (a) Pseudocapacitance or Capacitive faradaic storage (b) Intercalation pseudocapacitance (b) Non-capacitive faradaic storage [30] (Fig. 4a and Fig. 4b).

**(a) Pseudocapacitance or capacitive faradaic storage:** In pseudocapacitive materials like metal oxides ( $\text{MnO}_2$ ,  $\text{RuO}_2$  etc.), charge storage involves fast surface or near surface electron-transfer reactions, however, still they display capacitive behavior i.e. linear relationship between charge storage and applied voltage within a specific electrochemical window [27,31]. This is indicated by the square like curves in cyclic voltammetry (CVs).

**(b) Intercalation pseudocapacitance:** In some metal oxides such as  $\text{Nb}_2\text{O}_5$  [32], intercalation pseudocapacitance is observed, where faradaic charge-transfer occurs with no crystallographic phase change. Thus, charge storage occurs in the bulk of the material, where ions intercalate into the tunnels or layers of a redox-active material [33,34]. The kinetics are not diffusion-limited and instead are limited by surface processes such that it shows fast kinetic response like electric double-layer capacitors [35].

**(c) Non-capacitive faradaic charge storage:** The charge storage in some metal oxides (for example, Nickel Oxide, Cobalt oxides) involves fast surface reaction but amount of charge stored do not follow linear variation with voltage within their working electrochemical window. The faradaic processes in such battery-like electrodes are governed by the Nernst equation [31]. In Nernstian processes, electron transfer reaction occurs when the electrode potential reaches a particular value. Therefore, they display peak-shaped cyclic voltammetric scans (CVs) in comparison to square shaped CVs displayed by pseudocapacitive or carbonaceous materials [29]. Since these electrodes show battery-like behavior, they cannot be used to calculate capacitance using equations for EDLC and pseudocapacitance. Nevertheless, they can be combined with capacitive electrode material to form hybrids that achieve higher energy densities than the sum of its constituents [27, 36].

These different types of faradaic charge mechanisms of metal oxides can be explained by the band theory for semiconductors [36]. Fig. 4c shows a band model diagram for metals, semiconductors and insulators. In case of metals, no charges can be stored as there is complete overlap of energy states. While in case of insulators, redox active sites on electrode are non-interactive in nature, thus behaving like individual molecules. Therefore, localized electron transfer to these redox active sites happens in a narrow potential range [29].

So, in case materials showing non-capacitive faradaic behavior, the electron energy states are separated (localized) in isolated molecules or insulators (Fig.4c), such that electron injection or removal takes place in well separated redox sites. Since the redox centers are electronically isolated from each other they have fairly close energy states, which is corroborated by the peak shaped CVs [36]. While in case pseudocapacitive metal oxides, redox centers are interactive and energy states merge into a broad band. Due to de-localization of electrons, there is continuous electron transfer into (or from) each energy state over a wide range of potentials, as indicated by their rectangular CVs [29].

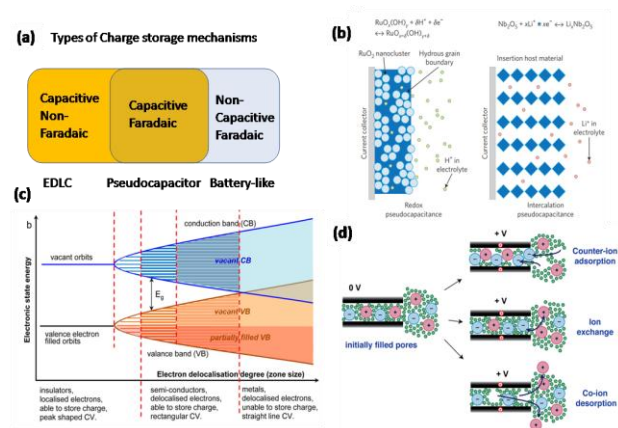


**Fig. 4.** (a) Schematic showing the classification of charge transfer mechanisms in supercapacitor; (b) Schematic illustration of charge transfer mechanism in pseudocapacitance and intercalation capacitance; (c) Band-gap diagram showing degree of delocalization for metals, semi-conductors, and insulators; (d) Mechanism of charging in nanopores [Fig. 3b, 3c, and 3d are reproduced with permissions from [36, 37, 38] respectively].

### Factors influencing the charge storage

Apart from the nature of charge storage mechanism, surface properties of electrode material and morphology of its micro- and nanostructures affect the electrochemical charge storage properties of supercapacitor. The most obvious is internal surface area as the capacitance is directly proportional to the surface area as indicated by equation 1. But not all the internal surface area is accessible to the electrolyte ions as interaction of ions with electrode material is influenced by pore size distribution, channel length etc. [38]. The type of charging mechanism also affects charge storage in

supercapacitors. The charging can happen in 3 different ways – (a) adsorption of counter-ions (traditional view of charging), (b) Ion exchange - counter-ion adsorption accompanied by simultaneous co-ion desorption from the pores, (where co-ions are the ions having same charge as the electrode), and (c) desorption of co-ions (**Fig. 4d**) [37]. But generally, charging involves combination of the different mechanisms. These mechanisms are dependent on the nature of the material and importantly, the nature of the surface, allowing us to tune surface with different functional moieties and morphologies. Apart from the type of charge storage mechanism there are many other factors that contribute to the overall performance of the supercapacitor such as - nature of the electrolyte (ionic conductivity, electrochemical stability, relative sizes and mobilities of co/counter-ions, ionic affinities towards electrode material), ion confinement effects at adsorption sites, cell configurations & charge-discharge dynamics etc., which are beyond the scope of the review and has been discussed elsewhere [25, 38, 37, 39, 40]. Yet, understanding of microscopic & mesoscale factors affecting charge storage can help us achieve higher charge storage capacity and optimum level of performance.

#### *Strategies to improve the charge storage in graphene-metal oxide nanocomposites*

The rationale behind graphene-metal oxide nanocomposite is to form a synergistic association by combining high energy density and capacitance of metal oxide with high power performance of graphene<sup>41</sup>. Combining the charge processes leads to synergistic effect of increase in capacitance, which can be done in three ways as follows:

- symmetrical supercapacitor consisting of same hybrid material at both the positive and negative electrodes.
- Asymmetrical hybrid supercapacitor consist of electrodes made up of two different materials, typically, graphene-metal oxide as positive electrode and graphene as negative electrode [42]. This increases the operational electrochemical window and specific capacitance in accordance with equation (3).
- battery-type hybrids, in which one of the electrode with battery-like behavior (non-faradaic non-capacitive (for example, in case of NiO, PbO<sub>2</sub> type of metal oxides) is paired with capacitive electrode and such supercapacitors are called as supercattery, [36]. They show high energy density but low cyclic stability [29].

Apart from the obvious benefits derived due to combined effect of the two charge transfer mechanisms, electrochemical performance is also enhanced due to following functional and structural enhancements:

- graphene acts as a 2D or 3D support for anchoring or uniform distribution of metal oxides
- graphene serves as a 3D conductive porous network improving electrical conductivity and charge transfer pathways;
- graphene suppresses the agglomeration and volume change in metal oxides during charge-discharge cycles;
- oxygen-

containing groups as well as modified functional groups on graphene ensures good wettability, ionic affinity and facilitates interfacial interactions between graphene and metal oxides. (v) metal oxides act as a spacer to reduce the agglomeration or re-stacking of graphene [43–45].

**Table 1:** List of various synthesis methods of graphene-metal oxide nanocomposite electrodes for supercapacitor applications.

Method of nanoparticle Synthesis	Types of Metal oxides used in nano composite electrodes	Particle size in nm	Processing temperature	Processing time	References
Solvothermal	SnO <sub>2</sub>	--	60°C	6h	50
Hydrothermal	Co <sub>3</sub> O <sub>4</sub>	20	180°C	1.5h	51
	Fe <sub>2</sub> O <sub>3</sub>	50-80	180°C	24	52
	Fe <sub>3</sub> O <sub>4</sub>	200-400	180°C	8h	53
	Mn <sub>3</sub> O <sub>4</sub> nanorods	5–30 nm in lengths, 100 nm- 1 μm long	120°C	4h	54
	NiO NPs	10-20	180°C	12h	55
	NiO flakes	--	180°C	12h	56
	TiO <sub>2</sub>	20-30	180°C	2h	57
	VO <sub>2</sub>	60-150	220°C	6h	58
	VO <sub>5</sub>	40	120°C	24	59
ZnO <sub>2</sub>	20-30	160°C	12h	60	
Electro-deposition	MnO <sub>2</sub>	10	RT	Stir till mixed	61
In situ reduction	Co <sub>3</sub> O <sub>4</sub>	5.8	100°C	3h	51
Dip coating	RuO <sub>2</sub>	~ 5	150°C	6h	62

#### **Graphene-metal oxide nanocomposites for supercapacitor applications**

Unlike its superior electrical and mechanical properties, graphene exhibits significantly poor electrochemical properties due to its inert basal planes, thus, graphene alone is unsuitable for applications in any charge-storage devices. On the other hand, metal oxides, such as, RuO<sub>2</sub>, MnO<sub>2</sub>, NiO, Co<sub>3</sub>O<sub>4</sub>, V<sub>2</sub>O<sub>5</sub>, Fe<sub>3</sub>O<sub>4</sub>, exhibit remarkable electrochemical properties and demonstrate their use in supercapacitor devices. However, the electrocatalytic properties of transition metal oxides are limited by their significantly high electrical resistivity which results in poor rate capability in any charge storage devices. On the other hand, pseudocapacitive materials commonly exhibit poor cyclic stability in long-term charge-discharge cycles due to their relatively poor structural stability, active loss of materials, and over-oxidative decomposition [46]. To address these issues effectively, two strategies have been employed to improve the supercapacitor performances, which are either by functionalizations of the electrode materials or fabrication of composite electrodes; or sometimes even combinations of both. In particular, composite electrodes have several advantages, including synergistic combination of electronic and ionic conductivities, high-surface area, controlled morphologies

with high specific capacitance and high energy density of metal oxides [47]. Several methods have been proposed for synthesizing various graphene-metal oxide nanocomposites such as: (a) hydrothermal and solvothermal methods which are cost-effective, low-temperature solution based approach to form graphene-metal oxide nanocomposites with diverse nano-architectures from 0 to 3 dimensions; (b) electrochemical method which involves either co-deposition of graphene-metal oxide nanocomposite or deposition of metal oxide nanostructures on graphene, driven by electric current; (c) in-situ approach which is a one-step, low-temperature, solution based approach for producing 3D graphene-metal oxide network [48, 49]. Metal oxide-Graphene nanocomposites with different types of metal oxides have been demonstrated using different chemical methods as tabulated in **Table 1**. Also, **Table 1** describes a brief overview of the diverse processes through which graphene-metal oxide composites can be synthesized with various particle size and other process parameters like temperature and time etc.

### Graphene-Manganese oxide nanocomposites

Amongst all metal oxide, manganese dioxide-graphene ( $\text{MnO}_2$ ) is widely investigated as electrode material for supercapacitor devices. The charge storage mechanism of a  $\text{MnO}_2$  electrode involves change of oxidation state of manganese (Mn) between III to IV. The pseudocapacitive behaviors of  $\text{MnO}_2$  thin films arises from the reversible insertion/extraction of electrolyte cations to balance the charge during reduction/oxidation of  $\text{Mn}^{3+}/\text{Mn}^{4+}$  [63, 64]. The hydrous regions in the electrode provide the kinetically facile sites needed for the charge-transfer reaction and diffusion of cations [65]. Similarly, the charge transfer mechanism of  $\text{Mn}_3\text{O}_4$  based electrodes follow the same charge transfer mechanism [66].  $\text{MnO}_2$  continues to develop interest owing to its desirable properties, like high theoretical specific capacitance (almost  $\sim 1340 \text{ Fg}^{-1}$ ) [67,68], environment friendly, and low cost [69]. However, intrinsically poor electrical conductivity of  $\text{MnO}_2$  leads towards lowering of the electrochemical properties. To enhance the supercapacitor performance, hybrid  $\text{MnO}_2/\text{graphene}$  nanostructures were developed for large-scale energy storage systems.

Yan *et al.* [70] developed a quick and room-temperature microwave-assisted method to synthesize  $\text{MnO}_2$ -graphene composite using  $\text{KMnO}_4$ . The composite at 78%  $\text{MnO}_2$  loading shows high specific capacitance of  $310 \text{ Fg}^{-1}$ , while capacitance retention was found to be 95.4%, after 15000 cycles with remarkably high stability at scan rate of  $500 \text{ mVs}^{-1}$ . This improved performance was attributed to well-dispersed small size  $\text{MnO}_2$  (5-10 nm) nanoparticles obtained in the composite. This homogeneously dispersed  $\text{MnO}_2$  on graphene membrane boosted the ion-buffering by reducing path length for cations during charge-discharge process, created fast electron transfer through graphene, and improved interfacial contact, hence reducing the voltage drop.

Ma *et al.* [69] showed that the hybrid of graphene fibers and  $\text{MnO}_2$  show promising flexible supercapacitor applications. Graphene fibers owing to their excellent mechanical and electrical properties are considered very suitable candidates for flexible electronic applications. However, graphene nanosheets aggregate due to strong  $\pi$ - $\pi$  interactions and tend to restack into graphite-like structure, which reduces the accessible surface area for ion adsorption/desorption and therefore leading to low specific capacitance and poor rate performance. To deal with those problems, a very simple, low cost and scalable wet-spinning method was developed to synthesizing  $\text{MnO}_2$  nanowires as the effective spacer in graphene fibers, which inhibited restacking and increased the specific surface area ( $139.9 \text{ m}^2 \text{ g}^{-1}$ ).

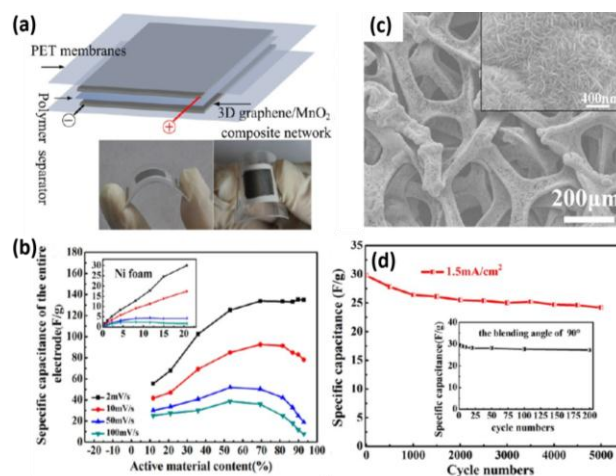


**Fig. 5.** (a) Schematic of the structure of graphene/ $\text{MnO}_2$  flexible supercapacitors and the two digital photographs show the flexible supercapacitors when bended; (b) SEM images of  $\text{MnO}_2$  on 3D graphene network; (c) Specific capacitance of the graphene/ $\text{MnO}_2$  electrode vs the content of active material ( $\text{MnO}_2$ ) at different scan rates; (d) Cyclic stability of the graphene/ $\text{MnO}_2$  composite electrodes at a current density of  $1.5 \text{ mA/cm}^2$  [Reproduced with permission from Ref. [71]].

The graphene nanosheets wrapped  $\text{MnO}_2$  nanowires provides an excellent electron transport through the fibrous nanostructure and facilitated the electrochemical utilization rate of  $\text{MnO}_2$  even at a high mass loading content of 40 wt%, all the while retaining their mechanical and electrical properties required for flexible supercapacitor applications. Thus, as constructed supercapacitor device using PVA- $\text{H}_3\text{PO}_4$  had been used as gel electrolyte shows very high volumetric capacitance ( $66.1 \text{ Fcm}^{-3}$ ) and excellent cycling stability (96% capacitance retention over 10000 cycles). Yongmin He *et al.* [71] electrochemically deposited  $\text{MnO}_2$  nanoparticles using a three-electrode setup, where the conductive 3D graphene network was used as the working electrode, a platinum electrode as the counter electrode, and a Ag/AgCl electrode as the reference electrode. The flexible electrode constructed shows electrochemical capacitance value of  $130 \text{ Fg}^{-1}$  and the cyclic performance retained 92% of its initial value even after 200 bending actions, indicating its excellent mechanical and flexible

properties (Fig. 5). Liu *et al.* developed a two-step hydrothermal technique in which first,  $\text{MnO}_2$ -rGO hybrids were synthesized by hydrothermal treatment, and the resulting composite was hydrothermally stabilized in carbon hollow nanofibers giving them very good stability until 5000 cycles. This added stability, helped to effectively control the problem of metal oxide leaching and graphene sheet aggregation. Graphene aerogels, known for high surface area and well-separated graphene monolayer, was prepared by functionalizing *p*-phenylenediamine (PPD) under hydrothermal conditions, and later,  $\text{MnO}_2$  NPs were grown uniformly using solution-phase deposition. Effect of cross-linker is evident by high energy density of  $26.2 \text{ Wh kg}^{-1}$  (at the power density of  $1000 \text{ W kg}^{-1}$ ), excellent cycle life showing 94 % capacitance retention after 5000 cycles [72]. Using a green chemistry route, Naderi Group [73], have shown room-temperature sonochemical route for depositing  $\text{MnO}_2$  on N-doped reduced graphene oxide (N-rGO). The doping of graphene, synergetic effect of hybrids and the uniform deposition of  $\text{MnO}_2$  aided by sonochemical method, all contributed to the high specific capacitance ( $522 \text{ Fg}^{-1}$  at  $2 \text{ mVs}^{-1}$ ) and high cyclic stability of 96.3% after 4000 CVs. Beyond,  $\text{MnO}_2$ ,  $\text{Mn}_3\text{O}_4$ , which is generally synthesized by Hydrazine, has shown comparable or even better electrochemical performance [54, 74].

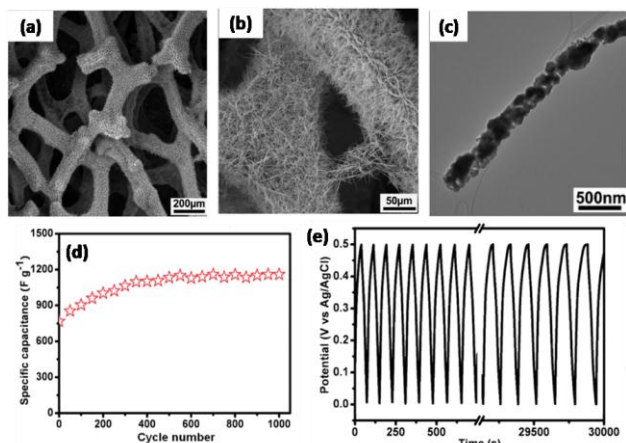


**Fig. 6.** (a) Scanning electron micrograph of (a and b) Graphene- $\text{Co}_3\text{O}_4$  nanocomposite foam at lower and higher magnification, respectively; (c) TEM image of  $\text{Co}_3\text{O}_4$  nanowires, (d) Cyclic performance and (e) Charge/discharge profile of graphene- $\text{Co}_3\text{O}_4$  composite electrode in supercapacitor device. [Reproduced with permissions from Ref 79].

### Graphene-Cobalt oxide nanocomposites

Apart from high theoretical capacitance ( $3560 \text{ Fg}^{-1}$ ) of cobalt-oxide based nanomaterial, it is abundant in nature and is touted to be environmental friendly [43, 75]. The pseudo capacitance of hydrous Cobalt oxides/hydroxides arises from the faradaic redox transitions of interfacial oxy-cation species [76]. The charge-discharge mechanism of cobalt oxide in alkaline electrolyte is explained by the formation of number of cobalt oxide phases with a transition between  $\text{Co(II)}$ ,  $\text{Co(III)}$  and  $\text{Co(IV)}$  oxidation

states, which involves formation of three redox couples  $-\text{Co(OH)}_2/\text{Co}_3\text{O}_4$ ,  $\text{Co}_3\text{O}_4/\text{CoOOH}$ , and  $\text{CoOOH}/\text{CoO}_2$  [77, 78].

Dong *et al.* [79] achieved high specific capacitance of  $1100 \text{ Fg}^{-1}$  by growing  $\text{Co}_3\text{O}_4$  nanowires on reduced graphene oxide (rGO) with improved structural morphology. Some inherent performance limitations in rGO such as aggregation & stacking due to  $\pi$ - $\pi$  interaction, interlayer contact resistance and defects and chemical moieties were overcome by synthesizing 3D highly porous graphene foam (Fig. 6a, 6b). The composite constructed by growing 200-300 nm thick, and several micrometre long  $\text{Co}_3\text{O}_4$  nanowires on graphene scaffold as shown in Fig. 6c. The nanocomposite showed remarkable capacitance retention above 25000 secs at high current density of  $10 \text{ Ag}^{-1}$  (Fig. 6d, 6e).

Liao *et al.* [75] addressed the electrocatalytic performance limitation arising due to  $\pi$ - $\pi$  stacking of graphene nanosheets by constructing a hybrid symmetric supercapacitor electrode of  $\text{Co}_3\text{O}_4$  nanoparticles on vertically aligned graphene nanosheet (VAGN) with its bottom fixed to the surface of the substrate (Fig. 7a, 7b). VAGN supported by the carbon fabric exhibited excellent support, which prevents restacking of the GNS. Thus, this architecture helps in reducing the internal resistance of the electrodes, which facilitates the faster diffusion of electrolyte towards the electrode. The whole surface of each carbon fiber was coated with the graphene sheets (as shown in Fig. 7c) followed by the deposition of  $\text{Co}_3\text{O}_4$  nanoparticles of  $\sim 5 \text{ nm}$  size using hydrothermal method. The solid-state symmetric supercapacitor constructed (as shown in Fig. 7d) from the VAGN hybrid material exhibits a high specific capacitance of  $580 \text{ Fg}^{-1}$ , good cycling ability showing 86.2% capacitance retention after 20,000 cycles. Consequently, the supercapacitor device based on VAGN electrode showed high energy density of  $80 \text{ Wh/kg}$ , and high-power density of  $20 \text{ kW/kg}$  at  $27 \text{ Wh/kg}$  (Fig. 7e, 7f).

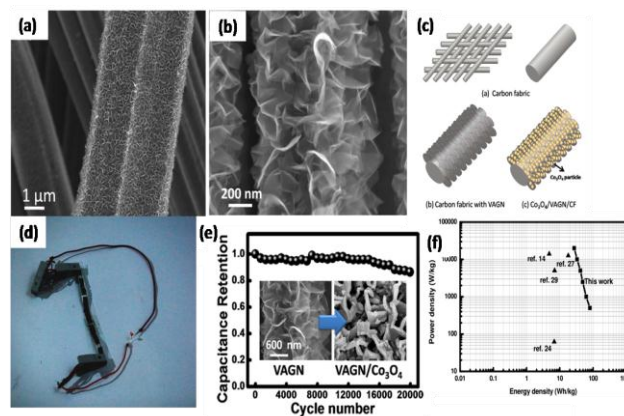


**Fig. 7.** (a, b) Carbon nanofibers coated with VAGN at different magnifications; (c) Schematic showing the synthesis method of VAGN- $\text{Co}_3\text{O}_4$  composites; (d) Actual solid state capacitor prototype; (e) Cycling stability (inset shows  $\text{Co}_3\text{O}_4$  on VAGN); (f) Ragone plot illustrating the performance of the VAGN- $\text{Co}_3\text{O}_4$  electrodes. [Reproduced with permissions from Ref 75].



In a search to develop one-step method for composite synthesis, microwave-exfoliated graphene oxide (MpEGO) was used as a substrate to grow  $\text{Co}_3\text{O}_4$  from a solution of cobalt acetate ultrasonic vibration [80]. The hybrid shows strong intercalation combined with high active surface area, which is reflected in its excellent cycle stability for 10,000 charges–discharge cycles and maximum power density and maximum energy density of 986.32 W/kg and 52.84 Wh/kg, respectively. Similarly, rGO prepared by modified hummers method was used to grow well dispersed  $\text{Co}_3\text{O}_4$  nanoparticles from cobalt nitrate hexa-hydrate metal salt and urea within a short time using microwave treatment (700W) [81]. In a study by Nguyen *et al.* [82], rGO- $\text{Co}_3\text{O}_4$  nanocomposite was synthesized using a facile and environment friendly method utilizing ammonia as a reducing agent. Apart from  $\text{Co}_3\text{O}_4$ , other forms of cobalt oxides such as CoO have been shown to exhibit comparable performance, and even excels in flexible applications [83]. CoO-graphene hybrid supercapacitors have been prepared by many methods such as hydrothermal treatment [84], electrospinning [83], chemical vapour deposition [85] etc.

### Graphene-iron oxide nanocomposites

Iron oxides attract as one of the potential electrode materials due its natural abundance, high thermal stability, low-toxicity, etc. Also, low manufacturing cost, suitable voltage window and high theoretical specific capacitance ( $\text{Fe}_2\text{O}_3$ -3625  $\text{Fg}^{-1}$ ,  $\text{FeOOH}$ - 2606  $\text{Fg}^{-1}$  and  $\text{Fe}_3\text{O}_4$ -2299  $\text{Fg}^{-1}$ ) make them suitable candidates for anode materials for supercapacitor devices [46, 86]. The pseudocapacitance of the Iron oxide –  $\text{Fe}_3\text{O}_4$  and  $\text{Fe}_2\text{O}_3$  are similar in nature [87], and arises from a reversible Fe(III)/Fe(II) redox couple, but the identity of the charge compensation in the pseudo capacitance reaction is yet [88, 89] to be fully understood [88, 89]. Wang *et al.* [90] has proposed that lithium intercalation in  $\text{Fe}_2\text{O}_3$  is dependent on the intrinsic crystal structure, where the lithium ions intercalate into the interlayer, the tunnels, and the holes through the crystal structure.

Qu *et al.* [91] demonstrated that the increase in electrochemical capacitive performance of 2D sandwich like  $\text{Fe}_3\text{O}_4$ -graphene nanocomposites are primarily due to the following: (i) maximizing electrochemical surface area by avoiding graphene re-stacking due to uniform surface deposition of  $\text{Fe}_3\text{O}_4$  and, (ii) synergistic effect of asymmetric capacitance value. Furthermore,  $\text{Fe}_3\text{O}_4$  nanorods were proposed to be formed by the dispersing nucleation of  $\text{FeOOH}$  nanorods on oxygen groups of GO followed by electrochemical cycling. The hybrid composite shows 2.5 times higher specific capacitance (304  $\text{Fg}^{-1}$ ) values, along with 1000 cycles capacitance retention for supercapacitor devices. Moreover,  $\text{Fe}_3\text{O}_4$ -graphene nanocomposites achieved higher power density despite of modest capacitance due to its negative working potential as compared to the other high-capacitive electrodes based on nickel oxides or cobalt oxides. In this regard, a supercapacitor-battery hybrid device was also

proposed by combining hydrothermally synthesized rGO- $\text{Fe}_3\text{O}_4$  nanocomposite as a negative electrode, and a 3D porous graphene-based carbon material as positive electrode material [92]. Thus,  $\text{Fe}_3\text{O}_4/\text{G}/3\text{D}$ -graphene hybrid demonstrated one of the highest reported values for hybrid supercapacitors of energy densities  $\sim 204$ – $65 \text{ Whkg}^{-1}$  over the power densities from 55 to 4600  $\text{Wkg}^{-1}$ . Ma *et al.* [93] reported an asymmetric supercapacitor device by combining both synergistic effect of metal oxide and graphene, as well as the nitrogen doped rGO, which showed specific capacitance of 267  $\text{Fg}^{-1}$  compared to pristine rGO (132  $\text{Fg}^{-1}$  at current density of 0.5  $\text{Ag}^{-1}$ ). Correspondingly, Liu *et al.* [46] developed one-pot solvothermal synthesis for  $\text{Fe}_2\text{O}_3$  nano-dots anchored on nitrogen-doped graphene sheets (Fig. 8a, 8b) The purpose of nitrogen doping was explained to increase the electrical conductivity of NG sheet and to improve the interfacial binding energy between  $\text{Fe}_2\text{O}_3$  NDs and NG sheets. Thus, the composite electrode performance in a SC device showed high specific capacitance (274  $\text{Fg}^{-1}$  at 1  $\text{Ag}^{-1}$ ), outstanding rate capability (140  $\text{Fg}^{-1}$  at 50  $\text{Ag}^{-1}$ ) and superior long-term cycling stability (75.3% after 100000 cycles at 5  $\text{Ag}^{-1}$ ) (Fig. 8c).

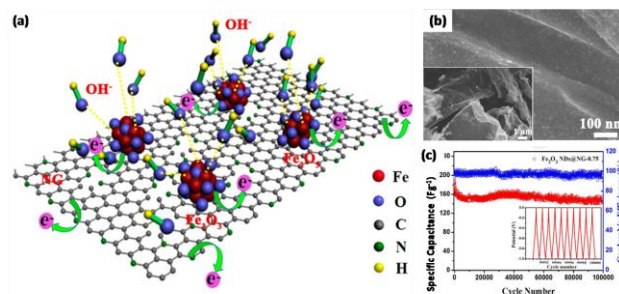


**Fig.8.** (a) Schematic diagram of surface faradaic redox reactions on the  $\text{Fe}_2\text{O}_3$  nanoparticles on Nitrogen doped graphene, (b) FESEM image of the graphene- $\text{Fe}_2\text{O}_3$  hybrids showing  $\text{Fe}_2\text{O}_3$  nanoparticles decorated on graphene nanosheets (inset shows hybrids at lower magnification) (c) Cyclic stability of the Graphene- $\text{Fe}_2\text{O}_3$  hybrid [Reproduced with permissions from Ref 46].

Recently, it was shown that application of cross-linkers like p-phenylenediamine (PPD) could address the common problem of graphene layer stacking. In particular, the use of cross linkers leads to doubling of surface area (388  $\text{m}^2\text{g}^{-1}$  as compared to 194  $\text{m}^2\text{g}^{-1}$  without cross-linker), much higher charge-discharge capacity and higher specific capacitance (445  $\text{Fg}^{-1}$ ) [94]. Similarly, Khattak *et al.* [95] and Song *et al.* [96] showed that enhancement in electrochemical performance of hybrid capacitor is possible by using graphene aerogel, which addresses limitations arising in available surface area due to graphene restacking.

### Graphene-Nickel oxide nanocomposites

Nickel Oxide (NiO) has been demonstrated as one of the potentially best electrode materials for supercapacitor devices. Also, NiO based electrodes are one of the highest reported theoretical specific capacitance of  $\sim 3750 \text{ Fg}^{-1}$

[88]. However, the performance of NiO was found to be limited due to its low electrical conductivity that gives rise to poor performance in the electrochemical devices [43]. The charge-discharge process involves formation of NiO-NiOOH redox couple, which involves the intercalation/deintercalation of protons [97, 98]. The pseudocapacitance is influenced by 3D micro-porous structure and presence of chemisorbed water, as loss of water beyond certain point causes decrease in specific capacitance [99]. Srivivasan *et al.* [100] investigated the charge-discharge mechanism in supercapacitor applications, where non-stoichiometric or defective structure plays a key role in the enhancement of its pseudocapacitive properties of NiO.

One of the earliest report on the supercapacitor properties of Nickel oxide was by Nam *et al.* [101] that shows good specific capacitance ( $277 \text{ Fg}^{-1}$ ) of the NiO<sub>x</sub> films prepared by the heat-treatment of Ni(OH)<sub>2</sub> films. Ren *et al.* [132] showed hydrothermal synthesis of various morphologies of NiO by varying pH values, of which honeycomb like NiO structures obtained at high pH displayed large specific area and pore volume. Asymmetric supercapacitor synthesized using NiO oxide as cathode and 3D porous graphene as anode displayed a good performance with a specific capacitance of  $74.4 \text{ Fg}^{-1}$ , energy density of  $23.25 \text{ Whkg}^{-1}$  and power density of  $9.3 \text{ kWkg}^{-1}$  and good cyclic stability (88% retention after 2000 cycles) (Fig 9). Zhao *et al.* [102] demonstrated the electro-catalytic properties of NiO by making synergistic nanocomposite with graphene where the process was reported as binder-free electrode preparation by growing NiO mesoporous nanowalls on rGO nanosheets on 3D nickel foams. Initially, a negatively charged GO nanosheets were electrochemically deposited on the Ni foam surface followed by the growth of Ni(OH)<sub>2</sub> using a low-temperature hydrothermal method. The growth occurs the mutual electrostatic interactions between the metal ions (Ni<sup>2+</sup>) and the possibly residual OH<sup>-</sup> and/or COO<sup>-</sup> groups in the electrochemically deposited and reduced graphene oxide. After the saturation adsorption on the rGO surface, Ni(OH)<sub>2</sub> self-assembly leads to the formation of a nanosheets-like structure on the surface of rGO in aqueous medium. Finally, a heat treatment process of the Ni(OH)<sub>2</sub>/graphene heterostructures at 400 °C in inert atmosphere for 2 h leads to the formation of dark-brown NiO-nanowalls/graphene nanocomposite. The Ni(OH)<sub>2</sub> nanowalls are composed of interconnected multilayer of stacked nanosheets on the surface of graphene coated on Ni foam. The 3D porous foam composite substrate of NiO-graphene nanocomposite provides efficient framework for electron collection and an electrolyte/ion diffusion through the active materials delivering high specific capacitance  $\sim 950 \text{ Fg}^{-1}$  at a current density of  $5 \text{ Ag}^{-1}$  with remarkable cycling stability.

In general, NiO nanoparticles are synthesized by thermal decomposition or refluxing of Ni(OH)<sub>2</sub>. However, to synthesize NiO-graphene hybrids, an one-step simple and facile electrochemical method has also been

introduced [103]. In this process, an alternating voltage was applied between a graphite rod and Ni flake to synthesize NiO quantum dots graphene hybrid flakes. The graphite rod surface was exfoliated due to alternating anodic and cathodic voltages, which OH<sup>-</sup> and H<sub>2</sub>O intercalate through the layered graphite structure. On the other hand, Ni-flakes was oxidized to form high valence NiO<sub>x</sub> or NiOOH, which was reduced and transformed into stable NiO nanocrystals on graphene. In an identical approach, NiO/graphene composites were also prepared on nickel foam via electrophoretic deposition (EPD) [103]. In EPD process, the preparation and modification of electrode was performed simultaneously where Ni<sup>2+</sup> ions deposited and bound with GO and form a NiO/graphene oxide composite. A high specific capacitance of  $1258 \text{ Fg}^{-1}$  at a current density of  $5 \text{ Ag}^{-1}$  was achieved with remarkable cycling stability (98.3% after 2000 cycles) for the SC devices using the EPD deposited NiO/graphene oxide electrodes. In another study, enhancement in electrochemical performance of NiO-graphene based hybrid electrodes was achieved with  $1328 \text{ Fg}^{-1}$  at a current density of  $1 \text{ Ag}^{-1}$  by using 3D porous graphene framework produced by the self-assembly of poly-methyl methacrylate (PMMA) and graphene oxide (GO), followed by adsorption of Ni precursor and high-temperature conversion to NiO [104]. To achieve better electrochemical stability for NiO-rGO composite, 3D graphene scaffolds grown on Ni foams by microwave plasma enhanced chemical vapor deposition (MPCVD) followed by hydrothermal synthesis of NiO nanoflakes on graphene scaffolds [56]. Supercapacitor device constructed with these electrodes showed high specific capacitance of  $\sim 1829 \text{ Fg}^{-1}$  at a current density of  $3 \text{ A g}^{-1}$  of 85% after 5000 cycles. In addition, NiO grown on graphene oxide sheets supported on metal organic framework [105] also showed ultimate performance in supercapacitor devices with specific capacitance of  $\sim 758 \text{ Fg}^{-1}$ , with energy density of  $37.8 \text{ Wh/kg}$  at a power density of  $227 \text{ W/kg}$ .

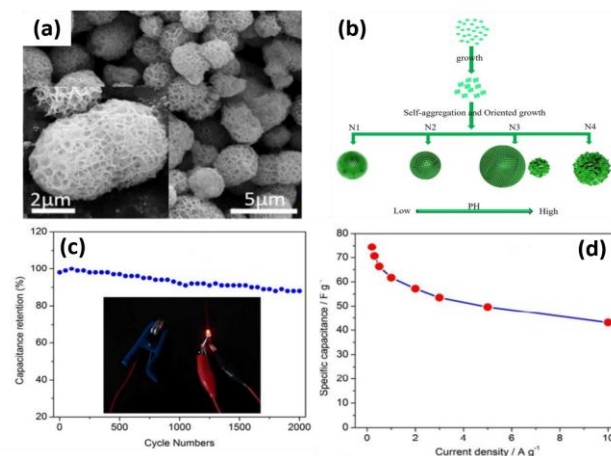


**Fig. 9.** (a) SEM image of NiO; (b) Schematic illustrating change in morphologies of NiO nanoparticles with pH; (c) Cyclic stability of NiO-graphene hybrid supercapacitor; (d) Specific capacitance at different current density. [Reproduced with permissions from Ref. 132].

### Graphene-vanadium oxide nanocomposites

Like other transition metal oxides, vanadium oxide ( $V_xO_y$ ;  $x=1-2$ ,  $y=1-5$ ) (VO) has several advantages for being used as potential electrocatalytic electrodes in SC devices. Specifically, VO exhibits low cost, abundant resources, layered structure, high energy density, comparable theoretical capacitance (290  $\text{mAhg}^{-1}$  and 1471  $\text{mAhg}^{-1}$  for cathode and anode respectively) and wide potential window arising from its multiple oxidation states [98]. The charge discharge performance of VO is influenced by pore size and percentage of hydration [99], while pseudo capacitance properties emerges from the reversible multiple oxidation states of different vanadium oxides like VO,  $\text{VO}_2$ ,  $\text{V}_2\text{O}_3$ , and  $\text{V}_2\text{O}_5$  [106].

Lee *et al.* [107] developed a facile, additive-free, rapid, low-temperature synthesis process for the graphene-decorated with  $\text{V}_2\text{O}_5$  nanobelts in aqueous medium. During the synthesis of nanocomposite,  $\text{V}_2\text{O}_5$  particles were converted into uniformly distributed nanobelts while simultaneously reducing GO to rGO. In this process, GO acts as a membrane as well as an oxidizing agent, which oxidizes the vanadium ions from  $\text{V}^{4+}$  to the  $\text{V}^{5+}$  during the reaction with GO. The resultant hybrid electrodes in a supercapacitor device showed a high capacitance (128.8  $\text{Fg}^{-1}$  at 0.5  $\text{Ag}^{-1}$ ) and long-term cycle life with the capacitance retention of 82% even after 5000 cycles [107].

Similarly, Wang *et al.* [58] demonstrated a low-temperature one-step hydrothermal process technique of synthesizing  $\text{VO}_2$  nanobelt-graphene nanocomposite. A nanocomposite hydrogel was formed with interwoven  $\text{VO}_2$  nanobelt on graphene sheet and the mechanism of formation of nanocomposite is shown in Fig. 10a. Such unique 3D hierarchical nanoarchitectures can offer (i) numerous channels, which facilitating rapid diffusion of electrolyte ions; (ii) a short diffusion length for electrolyte ions; and, (iii) a high electrical conductivity of the electrode due to the graphene network. The  $\text{VO}_2$  nanobelts with tens of micrometers length and typically 60–150 nm width was demonstrated in Fig. 10b, 10c. Thus, a hybrid electrode with synergistically new hierarchical architectures exhibit much higher electrocatalytic performance in supercapacitor (426  $\text{Fg}^{-1}$  at a current density of 1  $\text{Ag}^{-1}$ ) (Fig. 10d, 10e) and showed excellent long cycling stability [58].

Recently, Yilmaz *et al.* [108] reported a process for preparing freestanding, macroscopic, 3D network of  $\text{V}_2\text{O}_5$ -graphene aerogels composites. The process involved thiourea assisted cross-linking of functional groups (such as hydroxy, epoxide, and carboxy groups), which help inbuilding strong interfacial bonding with the rGO basal planes and  $\text{V}_2\text{O}_5$ . Following the similar strategy, several faster and one step hydrothermal synthesis methods have been reported so far. For example, (i) simultaneous hydrothermal reduction methodology was developed in suspension of  $\text{NH}_4\text{VO}_3$ , thiourea and graphite oxide (GO) nanosheets to prepare a  $\text{rGO}/\text{VO}_x \cdot n\text{H}_2\text{O}$  nanoplates [109]; (ii)  $\text{V}_2\text{O}_5$ -rGO composite was synthesized from one

pot hydrothermal synthesis [110]; (iii) a method of simultaneously reacting cetyltrimethylammonium bromide (CTAB) and rGO [106]; and (iv) vanadium pentoxide nanofibres (VNFs) grown on rGO nanosheets by in-situ growth [111].

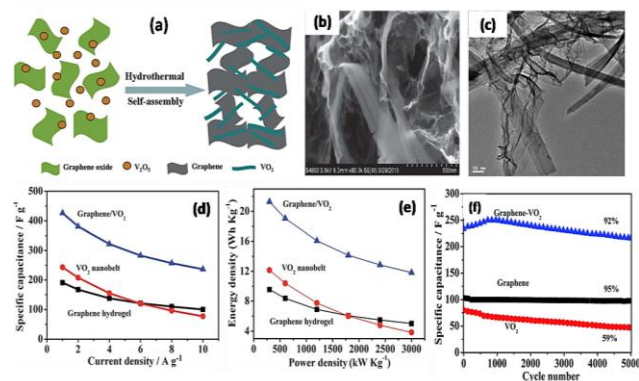


**Fig. 10.** (a) Schematic showing mechanism of composite synthesis; (b) SEM and (c) TEM image of the graphene foam- $\text{VO}_2$  nanobelt composites; (d), (e), & (f) illustrate the electrochemical performance comparison of the composite electrode in a supercapacitor device [Reprinted with permissions from Ref. 58].

### Graphene-Ruthenium Oxide nanocomposites

Ruthenium oxide ( $\text{RuO}_2$ ) is one of the potential electrocatalytic materials for supercapacitor electrode applications. The major advantages of  $\text{RuO}_2$  are of its wide potential window, highly reversible redox reactions, high proton conductivity, good thermal stability, long life cycle, metallic-type conductivity, and high rate capability. However, one primary drawback of  $\text{RuO}_2$  is its high cost. It was reported that about 90% of capacitive behavior of  $\text{RuO}_2$  was contributed by pseudocapacitance while only a small fraction (i.e. 10%) is contributed by EDL.  $\text{RuO}_2$  based electrocatalytic electrodes exhibits high theoretical capacitance of around 1358  $\text{Fg}^{-1}$  for supercapacitor devices [43] and this capability of accommodate inter-layer and inter-particle hydrous regions that allow smooth and faster protonic conduction leads to high power and energy density [27]. One of the studies on supercapacitor behavior of the  $\text{RuO}_2$  was conducted by Liu group [112] where they modelled the proton absorption-desorption mechanisms in acidic media and demonstrated the open-circuit potential recovery after sequential charge transients.

Zhang *et al.* [42] conducted a study of asymmetric supercapacitor of  $\text{RuO}_2$ -rGO and PANI-rGO (polyaniline) by comparing them with their symmetric counterparts. Apart from high power density (49.8  $\text{kWkg}^{-1}$ ), asymmetric capacitor showed almost double energy density compared to the rGO- $\text{RuO}_2$  symmetric capacitor. This reiterates importance of adopting asymmetric configuration to increase device performance while simultaneously increasing performance-to-cost ratio by reducing the amount of loadings of  $\text{RuO}_2$ . Wang *et al.* [113] constructed an asymmetric capacitor consisting of  $\text{Ni}(\text{OH})_2$ -graphene electrode with graphene- $\text{RuO}_2$

electrodes, which showed energy-power density (energy density of  $\sim 48$  Wh/kg at a power density of  $\sim 0.23$  kW/kg) of about 4 times higher than the individual constituents of RuO<sub>2</sub> composite [113]. In a unique two-step process, RuO<sub>2</sub>-graphene foam composite was synthesized where a conformal coating of RuO<sub>2</sub> nanoparticles were decorated on the few-layer graphene and CNT hybrid foam (GM) backbone. The resulting RGM electrode shows superior specific capacitance ( $502.78$  Fg<sup>-1</sup>) and extended operational voltage window of  $1.5$  V, which leads to an exceptionally high energy density of  $39.28$  Whkg<sup>-1</sup> and power density of  $128.01$  kW kg<sup>-1</sup>. In addition to the capacitance and energy density enhancement, the RGM SC also shows an excellent cycling stability of  $\sim 106\%$  capacitance retention over 8100 cycles [113].

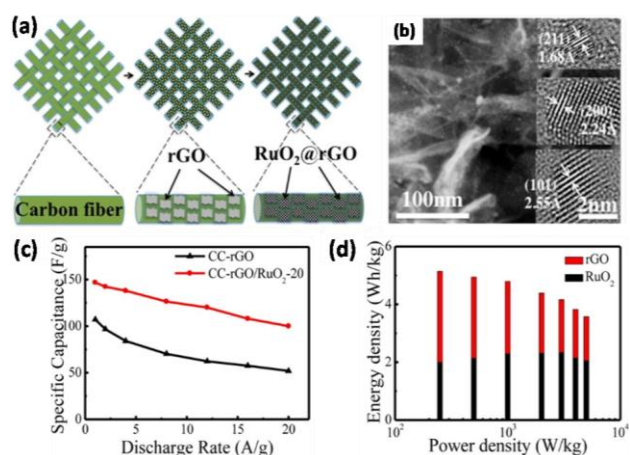


**Fig. 11.**(a) Schematic illustration of fabrication process of rGO/RuO<sub>2</sub> electrode, which demonstrates, rGO is electrochemically immobilized (ECI) on carbon cloth, followed by atomic layer deposition of RuO<sub>2</sub> on rGO, (b) Scanning transmission electron micrographs(STEM) of rGO/RuO<sub>2</sub> nanocomposite, (c) Specific capacitance of rGO/RuO<sub>2</sub> nanocomposite at different discharge current densities, (d) Ragone plot of energy density vs power density [Reprinted with permissions from Ref.<sup>[114]</sup>].

Yang *et al.* [114] developed two-step strategy to synthesize graphene-RuO<sub>2</sub> nanocomposites on carbon paper. First, graphene was electrochemically deposited on Carbon paper followed by atomic layer deposition (ALD) of RuO<sub>2</sub> nanoparticles on graphene nanosheets (Fig. 11a). Fig. 11b shows the scanning transmission electron microscopy (STEM) image (high-resolution transmission electron micrographs (HRTEM) are shown in the inset of Fig. 11b of graphene-RuO<sub>2</sub> nanoparticles. The inset figs. of Fig. 11b illustrates the HRTEM images of the nanocomposite with characteristics RuO<sub>2</sub> planes on graphene. The resultant electrodes show excellent cycling stability of  $\sim 92\%$  retention over 4000 cycles (Fig. 11c) and higher power and energy density (Fig. 11d). Recent improvements have been made to develop one-step facile methods for composite synthesis such as RuO<sub>2</sub>-reduced graphene oxide hydrogels prepared by a one-step hydrothermal

method [115], ultra-high specific capacitance ( $1139$  Fg<sup>-1</sup>), RuO<sub>2</sub>-graphene composite synthesized by laser-scribed RuO<sub>2</sub>-graphene nanocomposites into 3D electrodes [116], room-temperature electro-deposition of RuO<sub>2</sub> on rGO [117] etc.

### Graphene-other metal oxides based nanocomposites

Various other graphene/metal-oxides based nanocomposites have been explored for the use of preparing nanocomposite materials such as Nb<sub>2</sub>O<sub>5</sub> [32], SnO<sub>2</sub> [118], Bi<sub>2</sub>O<sub>3</sub> [119], IrO<sub>2</sub> [120], CeO<sub>2</sub> [121], MoO<sub>3</sub> [122], TiO<sub>2</sub> [57]. For example, TiO<sub>2</sub> and Cu<sub>x</sub>O, which are known to show only moderate electrochemical performance even in case of graphene hybrids but can serve as a viable alternative because of their natural abundance, well-established manufacturing processes, biocompatibility etc [27]. Some other transition metal oxides such as IrO<sub>2</sub>, MoO<sub>3</sub> and CeO<sub>2</sub> with graphene showed exceptional performance [121, 122] but their applications have been reported as limited owing to their cost. In such cases, several reports have been found proposing ternary composites of IrO<sub>2</sub>, MoO<sub>3</sub> and CeO<sub>2</sub> along with MnO<sub>2</sub>, Co<sub>3</sub>O<sub>4</sub> and graphene for synergistic effect. Various metal-oxide-graphene composites and their electrochemical performances have been listed in Table 2.

### Summary

In summary, we have reviewed and demonstrated a comprehensive outlook of recent advances on graphene-metal oxide nanocomposite based synergistic electrocatalytic electrodes and their extensive applications as supercapacitors. These synergistic nanostructures have been used successfully as supercapacitor electrodes due to their extraordinary double-layered charge storage properties. The performance of hybrid structures is unique compared to those of pure graphene, GO, rGO, or pure metal oxides. Considerable attention is given to those synergistic structure to obtain synergistic effects of both graphene and metal-oxides. The graphene in the hybrid-structure incorporate various advantages, including, high surface area ultra-thin thickness, excellent electrical and thermal conductivity, mechanical flexibility, while metal oxides improve high chemical functionality, and other electrochemical properties. Consequently, graphene can serve as an ideal 2D membrane for growing or assembling tiny nanoparticles/nanostructures with very distinct structures and precious morphologies. Also, in the hybrid structure, graphene can act as a 2D electrically conducting template for constituting a three-dimensional interconnected conductive porous network, which enhance the electrical conductivity as well as the charge transport kinetics through the pure-oxide nanoparticles. The other advantages of using hybrid structures are:

- 1) it can restrain the volume change and particle agglomeration of metal-oxides during the charge-discharge process;

**Table 2.** Comparison of electrochemical performance of various metal oxide-graphene nanocomposites.

Composite MOx – Graphene (arranged alphabetically)	Binder (Ratio is expressed as mass ratio)	Electrolyte	Cycles	Specific Capacitance F/g	Current Density A/g	Energy Density Wh/kg	Power Density kW/kg	Reference
Bi <sub>2</sub> O <sub>3</sub> rods-rGO	Acetylene Black + PTFE	6 M KOH	1000	1041	2	--	--	119
CeO <sub>2</sub> -Graphene	EA + CB + PTFE in a (8:1:1)	3M KOH	1000	18	1	--	208	121
Co <sub>3</sub> O <sub>4</sub> -3D-Graphene-	--	2.0 M KOH	1000	1100	10	--	--	79
Co <sub>3</sub> O <sub>4</sub> - Graphene	EA + CB+ 5% Nafion (80:15:5)	6 M KOH	300	415	3	--	--	124
Co <sub>3</sub> O <sub>4</sub> -Graphene	EA + PVDF (89:11) in NMP	2 M KOH	50	478	--	--	--	51
Fe <sub>2</sub> O <sub>3</sub> nanosheets-Graphene	EA + CB + PTFE (8:1:1)	--	1000	349	0.5	85	2.4	91
Fe <sub>2</sub> O <sub>3</sub> – Graphene	--	1 M Na <sub>2</sub> SO <sub>4</sub>	--	226	1	--	--	52
Fe <sub>3</sub> O <sub>4</sub> –Graphene	EA + CB+ PTFE (8:1:1)	1 M KOH	3000	220	0.5	--	--	53
N-doped-Graphne-foam-CNT-MnO <sub>2</sub>	--	1 M Na <sub>2</sub> SO <sub>4</sub>	15000	284	--	--	--	47
MnO <sub>2</sub> - Graphene	--	1 M Na <sub>2</sub> SO <sub>4</sub> Gel PVA/H <sub>3</sub> PO <sub>4</sub>	7000 cycles	267	0.2	18.64	12.6	125
PEDOT/MnO <sub>2</sub> sponge/Graphene	PEDOT	6 M KOH	10000	802.99	--	55.76		126
Standing (MnO <sub>2</sub> )-rGO hybrids	--	1 M Na <sub>2</sub> SO <sub>4</sub>	10000	1176	0.8	95	208.8	127
Mn <sub>3</sub> O <sub>4</sub> @N-doped carbon/graphene hybrids	Carbon Black + PTFE	1 M Na <sub>2</sub> SO <sub>4</sub>	2000	456	1	--	--	128
NiO- rGO	EA + AB + CG+ PTFE) 5:10:10:5)	6 M KOH	1100	576	1	--	--	129
NiO-3D graphene	--	1 M NaOH	5000	1829	3	138	5250	56
(RuO <sub>2</sub> -rGO)	EA + CB+ PTFE (75:20:5)	--	2500	400	0.3	6.8	49.8	42
RuO <sub>2</sub> -Graphene	--	2 M Li <sub>2</sub> SO <sub>4</sub>	8000	502.78	--	39.28	128.01	113
SnO <sub>2</sub> /Graphene	--	1 M H <sub>2</sub> SO <sub>4</sub>	--	43.4	--	--	--	118
TiO <sub>2</sub> -Graphene	--	0.5 M Na <sub>2</sub> SO <sub>4</sub>	2000	206.7	0.5	--	--	57
VO <sub>2</sub> nanobelt/ Graphene	--	0.5 M K <sub>2</sub> SO <sub>4</sub>	5000	426	1	21.3	--	58
V <sub>2</sub> O <sub>5</sub> nanowire graphene (flexible)	--	1 M (LiTFSI) in acetonitrile	70	80		38.8	455	59
rGO–Co-doped ZnO/PANI hybrid	ANN + PTFE +PANI	1 M H <sub>2</sub> SO <sub>4</sub>	--	515	--	370	3100	130
rGO/ZnO/poly(p-phenylenediamine)	EA + AB + (PVDF) (8:1:1)	1 M Na <sub>2</sub> SO <sub>4</sub>	1000	320	--	18.14	10kW	131

[Table Footnote: AB – Acetylene black; CB - carbon black; CG - Conducting Graphite; CMG - chemically modified graphene; CNT- Carbon nanotubes; CVD- Chemical vapour deposition; EA - Electroactive Material; LiTFSI - Lithium bis(tri-fluoromethanesulfonimide); NMP - N-methyl pyrrolidinone; PEDOT; PTFE - poly(tetrafluoroethylene); PVA – Poly vinyl alcohol; PVDF -Polyvinylidene fluoride; Pt = Platinum; rGO – reduced graphene oxide.]

- 2) oxygen-containing functional groups on GO, rGO assure good interfacial bonding and electrical contacts between graphene and metal oxides; and
- 3) metal-oxide nanoparticles inhibit the re-stacking of graphene layers, hence, continuous, porous, interconnected network structure is obtained with highest achievable power density and capacitance in supercapacitors. Thus, graphene-metal oxide hybrid-materials with all-inclusive remarkable properties turn into a suitable material for supercapacitor electrode applications.

### Perspective and challenges

A wide range of nano-hybrid structures have been demonstrated with various morphologies of metal oxides anchored with graphene, wrapped with graphene, encapsulated with graphene, layer-by-layer deposited with graphene, sandwiched with graphene, and mixed with graphene. Furthermore, these nano-hybrids with various nano-architectures with particle size, pore size and shape, conductive nano-channels, 2D to 3D interconnected network structures, spongy framework etc. have been demonstrated as well. This review primarily spotlighted various morphologies associated with novel architectures based on the nanohybrid materials, which greatly help in improving electrochemical performance of graphene-metal oxide nano-hybrid materials as electrodes with enhanced charge-storage capacity, increased rate capability, improved reliability of devices with cycling stability, and increased energy and power densities.

Although, this field of research has demonstrated significant amount of advancement in supercapacitor device performance and reliability, however, considerable amount of relevant challenges is still overlooked and needs to be resolved. These concerned issues can be described as follows:

1) **Chemistry and stoichiometry of metal oxides:** A thorough knowledge of chemistry of graphene and metal oxides, their interfacial bond formation, and surface charge-transfer properties are essential for getting a precise homogeneous nano-hybrid structure, thus, achieving better performance of the device. In particular, achieving a good control over surface chemistry, surface-stoichiometry, surface functionalization by modifying the covalent or non-covalent interface of graphene-metal oxide could help in improving the catalytic points of charge transfer, hence, improving supercapacitor performance.

2) **Heterogeneous interface formation:** Owing to their different crystal structure, graphene and metal-oxide forms heterogeneous interfaces in nano-hybrid structure. The heterogeneous interfaces inhibit electron transport resulting in deteriorating device performance. Thus, formations of a homogeneous interface between graphene and metal oxides are greatly desirable in order to achieve high performance supercapacitor device.

3) **Control over the nano-hybrid formation:** A strategic control over the morphology, stoichiometry, and phases of metal oxides nanostructures are required in order to ensure reproducibility and in-depth understanding of the structure–function relationships for supercapacitor applications. Similarly, a control of the texture and surface moieties of the graphene will possibly extend the potential use of graphene as a membrane template for the controlled growth of those oxide particle with smooth interface.

4) **Understanding electrochemical charge-transfer:** Understanding kinetics of electron transfer and mechanism of double layer formation will provide additional scope to implement device related issues and improve the rate of charge-discharge, capacitance, etc in a graphene-metal oxide based supercapacitors.

5) **Novel designs and novel process:** The development of novel designs and novel processes of graphene-metal oxide nanostructures require a combined aim to unfold new chemistry, controlled synthesis, and exceptional functionalities. The novel nano-hybrid materials with optimized properties, which is fundamental to improve the electrochemical performance of graphene-metal oxide nano-hybrid structures for supercapacitor devices.

6) **More commercially viable structures and processes:** Since, the development of supercapacitor technology was inclined towards its use in portable electronics and wearable devices, however, a real-life light-weight, thin, flexible devices are still under demand. In this regard, graphene shows some extraordinary promises owing to its unusual properties like, ultra-thin, light weight, high electrical conductivity associated with good thermal and mechanical properties. Another exclusive property of graphene is that it can identically perform even in bending or twisting conditions, thus this is an added advantage of graphene to be used for supercapacitor technology. Therefore, graphene-metal oxide nano-hybrids have displayed enormous possibilities for building up high-energy, high-power density supercapacitors with other functionalities. However, more commercially viable structure and processes are yet to discover for bringing this technology for next-level of commercialized devices.

To sum it all, a considerable amount of future efforts need to be incorporated on the controlled synthesis of the graphene-metal oxide based nanocomposites by controlling their surface structure, morphology, particle size, surface area, pore size, and 2D to 3D architectures in order to achieve the best functionality of the hybrid nanostructure. It can be assured that with systematic in-detail study on the graphene-metal oxide based electrodes could open up several other novel device applications for next-generation energy storage system.

### Acknowledgement

A part of this work is partly supported by funding from Dr. Das's Early Career Award from SERB/DST (Grant No: ECR/2016/001112), Govt. of India. Dr. Das also acknowledge the "Center for Energy Research and Development" IIT (BHU) for providing some funding for this work. All author of this work is gratefully acknowledged Director, IIT (BHU) for providing the facilities and monetary support for this work.

## References:

1. Stankovich S, Dikin DA, Dommett GHB, et al. Graphene-based composite materials. *Nature*. 2006;442(7100):282-286. DOI: <http://dx.doi.org/10.1038/nature04969>.
2. Das S, Sudhagar P, Kang YS, Choi W. Synthesis and Characterization of Graphene. In: *Carbon Nanomaterials for Advanced Energy Systems*. John Wiley & Sons, Inc; 2015:85-131. DOI: [10.1002/9781118980989.ch3](https://doi.org/10.1002/9781118980989.ch3)
3. Park H, Chang S, Smith M, Gradečak S, Kong J. Interface engineering of graphene for universal applications as both anode and cathode in organic photovoltaics. *Sci Rep*. 2013;3(1):1581. DOI: [10.1038/srep01581](https://doi.org/10.1038/srep01581)
4. Choi D, Kuru C, Choi C, et al. Nanopatterned Graphene Field Effect Transistor Fabricated Using Block Co-polymer Lithography. *Mater Res Lett*. 2014;2(3):131-139. DOI: [10.1080/21663831.2013.876676](https://doi.org/10.1080/21663831.2013.876676)
5. Das S, Lahiri I, Chiwon Kang, Wonbong Choi. Engineering carbon nanomaterials for future applications: Energy and bio-sensor. *Proc SPIE - Int Soc Opt Eng*. 2011;8031:1-11. DOI: [10.1117/12.883743](https://doi.org/10.1117/12.883743).
6. Das S, Sudhagar P, Verma V, et al. Amplifying Charge-Transfer Characteristics of Graphene for Triiodide Reduction in Dye-Sensitized Solar Cells. *Adv Funct Mater*. 2011;21(19):3729-3736. DOI: [10.1002/adfm.201101191](https://doi.org/10.1002/adfm.201101191)
7. Das S, Seelaboyina R, Verma V, et al. Synthesis and characterization of self-organized multilayered graphene-carbon nanotube hybrid films. *J Mater Chem*. 2011;21(20):7289. DOI: [10.1039/c1jm10316d](https://doi.org/10.1039/c1jm10316d)
8. Devadoss A, Sudhagar P, Das S, et al. Synergistic Metal-Metal Oxide Nanoparticles Supported Electrocatalytic Graphene for Improved Photoelectrochemical Glucose Oxidation. *ACS Appl Mater Interfaces*. 2014;6(7):4864-4871. DOI: [10.1021/am4058925](https://doi.org/10.1021/am4058925)
9. Das S, Sudhagar P, Nagarajan S, et al. Synthesis of graphene-CoS electro-catalytic electrodes for dye sensitized solar cells. *Carbon N Y*. 2012;50(13):4815-4821. DOI: [10.1016/j.carbon.2012.06.006](https://doi.org/10.1016/j.carbon.2012.06.006).
10. Das S, Sudhagar P, Ito E, et al. Effect of HNO<sub>3</sub> functionalization on large scale graphene for enhanced tri-iodide reduction in dye-sensitized solar cells. *J Mater Chem*. 2012;22(38):20490. DOI: [10.1039/c2jm32481d](https://doi.org/10.1039/c2jm32481d).
11. Polat EO, Balci O, Kakenov N, Uzlu HB, Kocabas C, Dahiya R. Synthesis of Large Area Graphene for High Performance in Flexible Optoelectronic Devices. *Sci Rep*. 2015;5(1):16744. DOI: [10.1038/srep16744](https://doi.org/10.1038/srep16744).
12. Das S, Choi W. Graphene Synthesis. In: *Graphene*. Nanomaterials and their Applications. CRC Press; 2011:27-64. DOI: [10.1201/b11259-3](https://doi.org/10.1201/b11259-3).
13. Diamond W Do. Mass production of high quality graphene: An analysis of worldwide patents. *Juin*, 28:1-6. <http://www.nanowerk.com/spotlight/spotid=25744.php>. Published 2012. Accessed July 13, 2017.
14. Cai M, Thorpe D, Adamson DH, Schniepp HC. Methods of graphite exfoliation. *J Mater Chem*. 2012;22(48):2492. DOI: [10.1039/c2jm34517j](https://doi.org/10.1039/c2jm34517j).
15. Viculis LM. A Chemical Route to Carbon Nanoscrolls. *Science (80)*. 2003;299(5611):1361-1361. DOI: [10.1126/science.1078842](https://doi.org/10.1126/science.1078842).
16. Liu M, Shi M, Lu W, Zhu D, Li L, Gan L. Core-shell reduced graphene oxide/MnOx@carbon hollow nanospheres for high performance supercapacitor electrodes. *ChemEng J*. 2017;313:518-526. DOI: [10.1016/j.cej.2016.12.091](https://doi.org/10.1016/j.cej.2016.12.091).
17. Hummers WS, Offeman RE. Preparation of Graphitic Oxide. *J Am Chem Soc*. 1958;80(6):1339-1339. DOI: [10.1021/ja01539a017](https://doi.org/10.1021/ja01539a017).
18. Park S, Ruoff RS. Chemical methods for the production of graphenes. *Nat Nanotechnol*. 2009;4(4):217-224. DOI: [10.1038/nnano.2009.58](https://doi.org/10.1038/nnano.2009.58).
19. Stankovich S, Dikin DA, Piner RD, et al. Synthesis of graphene-based nanosheets via chemical reduction of exfoliated graphite oxide. *Carbon N Y*. 2007;45(7):1558-1565. DOI: [10.1016/j.carbon.2007.02.034](https://doi.org/10.1016/j.carbon.2007.02.034).
20. Marcano DC, Kosynkin D V, Berlin JM, et al. Improved Synthesis of Graphene Oxide. *ACS Nano*. 2010;4(8):4806-4814. DOI: [10.1021/nn1006368](https://doi.org/10.1021/nn1006368).
21. Zhu Y, Murali S, Cai W, et al. Graphene and graphene oxide: Synthesis, properties, and applications. *Adv Mater*. 2010; 22(35): 3906-3924. DOI: [10.1002/adma.201001068](https://doi.org/10.1002/adma.201001068).
22. Yang Z, Zheng Q, Qiu H, Li J, Yang J. A simple method for the reduction of graphene oxide by sodium borohydride with CaCl<sub>2</sub> as a catalyst. *New Carbon Mater*. 2015;30(1):41-47. DOI: [10.1016/S1872-5805\(15\)60174-3](https://doi.org/10.1016/S1872-5805(15)60174-3).
23. Mattevi C, Kim H, Chhowalla M, et al. A review of chemical vapour deposition of graphene on copper. *J Mater Chem*. 2011;21(10):3324-3334. DOI: [10.1039/C0JM02126A](https://doi.org/10.1039/C0JM02126A).
24. Zheng Q, Kim J-K. Synthesis, Structure, and Properties of Graphene and Graphene Oxide. In: *Graphene for Transparent Conductors*. New York, NY: Springer New York; 2015:29-94. DOI: [10.1007/978-1-4939-2769-2\\_2](https://doi.org/10.1007/978-1-4939-2769-2_2).
25. Burke A. Ultracapacitors: Why, how, and where is the technology. *J Power Sources*. 2000;91(1):37-50. DOI: [10.1016/S0378-7753\(00\)00485-7](https://doi.org/10.1016/S0378-7753(00)00485-7).
26. Kötz R, Carlen M. Principles and applications of electrochemical capacitors. *Electrochim Acta*. 2000;45(15):2483-2498. DOI: [10.1016/S0013-4686\(00\)00354-6](https://doi.org/10.1016/S0013-4686(00)00354-6).
27. Gonzalez A, Goikolea E, Barrena JA, Mysyk R. Review on supercapacitors: Technologies and materials. *Renew Sustain Energy Rev*. 2016;58:1189-1206. DOI: [10.1016/j.rser.2015.12.249](https://doi.org/10.1016/j.rser.2015.12.249).
28. Simon P, Gogotsi Y. Materials for electrochemical capacitors. *Nat Mater*. 2008;7(11):845-854. DOI: [10.1038/nmat2297](https://doi.org/10.1038/nmat2297).
29. Guan L, Yu L, Chen GZ. Capacitive and non-capacitive faradaic charge storage. *Electrochim Acta*. 2016;206:464-478. DOI: [10.1016/j.electacta.2016.01.213](https://doi.org/10.1016/j.electacta.2016.01.213).
30. Akinwolemiwa B, Wei C, Chen GZ. Mechanisms and Designs of Asymmetrical Electrochemical Capacitors. *Electrochim Acta*. 2017; 247: 344-357. DOI: [10.1016/j.electacta.2017.06.088](https://doi.org/10.1016/j.electacta.2017.06.088).
31. Brousse T, Belanger D, Long JW. To Be or Not To Be Pseudocapacitive? *J Electrochem Soc*. 2015;162(5):5185-5189. DOI: [10.1149/2.0201505jes](https://doi.org/10.1149/2.0201505jes).
32. Kong L, Zhang C, Wang J, Qiao W, Ling L, Long D. Free-Standing T-Nb<sub>2</sub>O<sub>5</sub>/Graphene Composite Papers with Ultrahigh Gravimetric/Volumetric Capacitance for Li-Ion Intercalation Pseudocapacitor. *ACS Nano*. 2015;9(11):11200-11208. DOI: [10.1021/acsnano.5b04737](https://doi.org/10.1021/acsnano.5b04737). Yoo HD, Li Y, Liang Y, Lan Y, Wang F, Yao Y. Intercalation Pseudocapacitance of Exfoliated Molybdenum Disulfide for Ultrafast Energy Storage. *ChemNanoMat*. 2016;2(7):688-691. DOI: [10.1002/cnma.201600117](https://doi.org/10.1002/cnma.201600117).
34. Lubimtsev AA, Kent PRC, Sumpter BG, Ganesh P. Understanding the origin of high-rate intercalation pseudocapacitance in Nb<sub>2</sub>O<sub>5</sub> crystals. *J Mater Chem A*. 2013;1(47):14951. DOI: [10.1039/c3ta13316h](https://doi.org/10.1039/c3ta13316h).
35. Augustyn V, Come J, Lowe MA, et al. High-rate electrochemical energy storage through Li<sup>+</sup> intercalation pseudocapacitance. *Nat Mater*. 2013;12(6):518-522. DOI: [10.1038/nmat3601](https://doi.org/10.1038/nmat3601)
36. Augustyn V, Simon P, Dunn B. Pseudocapacitive oxide materials for high-rate electrochemical energy storage. *Energy Environ Sci*. 2014;7(5):1597. DOI: [10.1039/c3ee44164d](https://doi.org/10.1039/c3ee44164d).
37. Chen GZ. Supercapacitor and supercapattery as emerging electrochemical energy stores. *Int Mater Rev*. 2017;62(4):173-202. DOI: [10.1080/09506608.2016.1240914](https://doi.org/10.1080/09506608.2016.1240914).
38. Griffin JM, Forse AC, Wang H, et al. Ion counting in supercapacitor electrodes using NMR spectroscopy. *Faraday Discuss*. 2014;176:49-68. DOI: [10.1039/C4FD00138A](https://doi.org/10.1039/C4FD00138A).
39. Merlet C, Péan C, Rotenberg B, et al. Highly confined ions store charge more efficiently in supercapacitors. *Nat Commun*. 2013;4:2701. DOI: [10.1038/ncomms3701](https://doi.org/10.1038/ncomms3701).

40. Deschamps M, Gilbert E, Azais P, et al. Exploring electrolyte organization in supercapacitor electrodes with solid-state NMR. *Nat Mater.* 2013;12(4):351-358.  
DOI:10.1038/nmat3567.
41. Wu Z-S, Zhou G, Yin L-C, Ren W, Li F, Cheng H-M. Graphene/metal oxide composite electrode materials for energy storage. *Nano Energy.* 2012;1(1):107-131.  
DOI:10.1016/j.nanoen.2011.11.001.
42. Zhang J, Jiang J, Li H, Zhao XS. A high-performance asymmetric supercapacitor fabricated with graphene-based electrodes. *Energy Environ Sci.* 2011;4(10):4009.  
DOI:10.1039/c1ee01354h.
43. Lokhande VC, Lokhande AC, Lokhande CD, Kim JH, Ji T. Supercapacitive composite metal oxide electrodes formed with carbon, metal oxides and conducting polymers. *J Alloys Compd.* 2016;682:381-403.  
DOI:10.1016/j.jallcom.2016.04.242.
44. Jeong GH, Baek S, Lee S, Kim SW. Metal Oxide/Graphene Composites for Supercapacitive Electrode Materials. *Chem - An Asian J.* 2016;11(7):949-964.  
DOI:10.1002/asia.201501072.
45. Chen J, Li C, Shi G. Graphene Materials for Electrochemical Capacitors. *J Phys Chem Lett.* 2013;4:1244-1253.  
DOI:10.1021/jz400160k.
46. Liu L, Lang J, Zhang P, Hu B, Yan X. Facile Synthesis of Fe<sub>2</sub>O<sub>3</sub> Nano-Dots@Nitrogen-Doped Graphene for Supercapacitor Electrode with Ultralong Cycle Life in KOH Electrolyte. *ACS Appl Mater Interfaces.* 2016;8(14):9335-9344.  
DOI:10.1021/acsami.6b00225.
47. Cheng T, Yu B, Cao L, et al. Synthesis and loading-dependent characteristics of nitrogen-doped graphene foam/carbon nanotube/manganese oxide ternary composite electrodes for high performance supercapacitors. *J Colloid Interface Sci.* 2017; 501:1-10.  
DOI:10.1016/j.jcis.2017.04.039.
48. Majeed A, Ullah W, Anwar AW, et al. Graphene-metal oxides/hydroxide nanocomposite materials: Fabrication advancements and supercapacitive performance. *J Alloys Compd.* 2016; 671:1-10.  
DOI:10.1016/j.jallcom.2015.12.083.
49. Chen W, Li S, Chen C, Yan L. Self-assembly and embedding of nanoparticles by in situ reduced graphene for preparation of a 3D graphene/nanoparticle aerogel. *Adv Mater.* 2011;23(47):5679-5683.  
DOI:10.1002/adma.201102838.
50. Li F, Song J, Yang H, et al. One-step synthesis of graphene / SnO<sub>2</sub> nanocomposites and its application in electrochemical supercapacitors. *Nanotechnology.* 2009;20(45):455602.  
DOI:10.1088/0957-4484/20/45/455602.
51. He G, Li J, Chen H, et al. Hydrothermal Preparation of Co<sub>3</sub>O<sub>4</sub>@graphene Nanocomposite for Supercapacitor with Enhanced Capacitive Performance. Vol 82.; 2012.  
DOI:10.1016/j.matlet.2012.05.048.
52. Wang Z, Ma C, Wang H, Liu Z, Hao Z. Facilely synthesized Fe<sub>2</sub>O<sub>3</sub>-graphene nanocomposite as novel electrode materials for supercapacitors with high performance. *J Alloys Compd.* 2013; 552: 486-491.  
DOI:10.1016/j.jallcom.2012.11.071.
53. Wang Q, Jiao L, Du H, Wang Y, Yuan H. Fe<sub>3</sub>O<sub>4</sub> nanoparticles grown on graphene as advanced electrode materials for supercapacitors. *J Power Sources.* 2014;245:101-106.  
DOI:10.1016/j.jpowsour.2013.06.035.
54. Lee JW, Hall AS, Kim J-D, Mallouk TE. A Facile and Template-Free Hydrothermal Synthesis of Mn<sub>3</sub>O<sub>4</sub> Nanorods on Graphene Sheets for Supercapacitor Electrodes with Long Cycle Stability. *Chem Mater.* 2012;24(6):1158-1164.  
DOI:10.1021/cm203697w.
55. Yang Y-Y, Hu Z-A, Zhang Z-Y, et al. Reduced graphene oxide-nickel oxide composites with high electrochemical capacitive performance. *Mater Chem Phys.* 2012;133(1):363-368.  
DOI:10.1016/j.matchemphys.2012.01.039.
56. Wang C, Xu J, Yuen MF, et al. Hierarchical composite electrodes of nickel oxide nanoflake 3D graphene for high-performance pseudocapacitors. *Adv Funct Mater.* 2014;24(40):6372-6380.  
DOI:10.1002/adfm.201401216.
57. Zhang Z, Xiao F, Guo Y, Wang S, Liu Y. One-Pot Self-Assembled Three-Dimensional TiO<sub>2</sub> - Graphene Hydrogel with Improved Adsorption Capacities and Photocatalytic and Electrochemical Activities.2013;5:2227-2233.  
DOI:10.1021/am303299r
58. Wang H, Yi H, Chen X, Wang X. One-step strategy to three-dimensional graphene/VO<sub>2</sub> nanobelt composite hydrogels for high performance supercapacitors. *J Mater Chem A.* 2014;2(4):1165-1173.  
DOI:10.1039/C3TA13932H.
59. Perera SD, Liyanage AD, Nijem N, Ferraris JP, Chabal YJ, Balkus KJ. Vanadium oxide nanowire - Graphene binder free nanocomposite paper electrodes for supercapacitors: A facile green approach. *J Power Sources.* 2013;230:130-137.  
DOI:10.1016/j.jpowsour.2012.11.118.
60. Li Z, Zhou Z, Yun G, Shi K, Lv X, Yang B. High-performance solid-state supercapacitors based on graphene-ZnO hybrid nanocomposites. 2013;8(1):473.  
DOI:10.1186/1556-276X-8-473
61. Cheng Q, Tang J, Ma J, Zhang H, Shinya N, Qin L-C. Graphene and nanostructured MnO<sub>2</sub> composite electrodes for supercapacitors. *Carbon N Y.* 2011;49(9):2917-2925.  
DOI:10.1016/j.carbon.2011.02.068.
62. Wang W, Guo S, Lee I, et al. Hydrous Ruthenium Oxide Nanoparticles Anchored to Graphene and Carbon Nanotube Hybrid Foam for Supercapacitors. *Sci Rep.* 2014;4(ii):9-14.  
DOI:10.1038/srep04452.
63. Kuo S-L, Wu N-L. Investigation of Pseudocapacitive Charge-Storage Reaction of MnO<sub>2</sub>·nH<sub>2</sub>O Supercapacitors in Aqueous Electrolytes. *J Electrochem Soc.* 2006;153(7):A1317.  
DOI:10.1149/1.2197667.
64. Kozawa A, Powers RA. The Manganese Dioxide Electrode in Alkaline Electrolyte; The Electron-Proton Mechanism for the Discharge Process from MnO<sub>2</sub> to MnO<sub>1.5</sub>. *J Electrochem Soc.* 1966;113(1):870-878.  
DOI: 10.1149/1.2424145
65. Ghaemi M, Ataheerian F, Zolfaghari A, Jafari SM. Charge storage mechanism of sonochemically prepared MnO<sub>2</sub> as supercapacitor electrode: Effects of physisorbed water and proton conduction. *Electrochim Acta.* 2008;53(14):4607-4614.  
DOI:10.1016/j.electacta.2007.12.040.
66. An G, Yu P, Xiao M, et al. Low-temperature synthesis of Mn<sub>3</sub>O<sub>4</sub> nanoparticles loaded on multi-walled carbon nanotubes and their application in electrochemical capacitors. *Nanotechnology.* 2008;19(27):275709.  
DOI:10.1088/0957-4484/19/27/275709.
67. Toupin M, Brousse T, Blanger D, Be D. Charge Storage Mechanism of MnO Electrode Used in Aqueous Electrochemical Capacitor Charge Storage Mechanism of MnO<sub>2</sub> Electrode Used in Aqueous Electrochemical Capacitor. *Chem Mater.* 2004; (9):3184-3190.  
DOI:10.1021/cm049649j.
68. Devaraj S, Munichandraiah N. High Capacitance of Electrodeposited MnO<sub>2</sub> by the Effect of a Surface-Active Agent. *Electrochem Solid-State Lett.* 2005;8(7):A373.  
DOI:10.1149/1.1922869.
69. Ma W, Chen S, Yang S, et al. Hierarchical MnO<sub>2</sub> nanowire/graphene hybrid fibers with excellent electrochemical performance for flexible solid-state supercapacitors. *J Power Sources.* 2016;306:481-488.  
DOI:10.1016/j.jpowsour.2015.12.063.
70. Yan J, Fan Z, Wei T, Qian W, Zhang M, Wei F. Fast and reversible surface redox reaction of graphene-MnO<sub>2</sub> composites as supercapacitor electrodes. *Carbon N Y.* 2010;48(13):3825-3833.  
DOI:10.1016/j.carbon.2010.06.047.
71. He Y, Chen W, Li X, et al. Freestanding three-dimensional graphene/MnO<sub>2</sub> composite networks as ultralight and flexible supercapacitor electrodes. *ACS Nano.* 2013;7(1):174-182.  
DOI:10.1021/nn304833s.
72. Gholipour-Ranjbar H, Ganjali MR, Norouzi P, Naderi HR. Functionalized graphene aerogel with p-phenylenediamine and its composite with porous MnO<sub>2</sub>: investigating the effect of functionalizing agent on supercapacitive performance. *J Mater Sci*



- Mater Electron.* 2016;27(10):10163-10172.  
**DOI:**[10.1007/s10854-016-5093-1](https://doi.org/10.1007/s10854-016-5093-1).
73. Naderi HR, Norouzi P, Ganjali MR. Electrochemical study of a novel high performance supercapacitor based on MnO<sub>2</sub>/nitrogen-doped graphene nanocomposite. *Appl Surf Sci.* 2016;366:552-560.  
**DOI:**[10.1016/j.apsusc.2016.01.058](https://doi.org/10.1016/j.apsusc.2016.01.058).
74. Zhang N, Qi P, Ding Y-H, Huang C-J, Zhang J-Y, Fang Y-Z. A novel reduction synthesis of the graphene/Mn<sub>3</sub>O<sub>4</sub> nanocomposite for supercapacitors. *J Solid State Chem.* 2016;237:378-384.  
**DOI:**[10.1016/j.jssc.2016.02.049](https://doi.org/10.1016/j.jssc.2016.02.049).
75. Liao Q, Li N, Jin S, Yang G, Wang C. All-Solid-State Symmetric Supercapacitor Based on Co<sub>3</sub>O<sub>4</sub> Nanoparticles on Vertically Aligned Graphene. *ACS Nano.* 2015;9(5):5310-5317.  
**DOI:**[10.1021/acsnano.5b00821](https://doi.org/10.1021/acsnano.5b00821).
76. Wang X-F, Ruan D-B, You Z. Pseudo-capacitive behavior of cobalt hydroxide/carbon nanotubes composite prepared by cathodic deposition. *Chinese J Chem Phys.* 2006;19(6):499-505-i.  
**DOI:**[10.1360/cjcp2006.19\(6\).499.7](https://doi.org/10.1360/cjcp2006.19(6).499.7).
77. Casella IG, Gatta M. Study of the electrochemical deposition and properties of cobalt oxide species in citrate alkaline solutions. *J Electroanal Chem.* 2002;534(1):31-38.  
**DOI:**[10.1016/S0022-0728\(02\)01100-2](https://doi.org/10.1016/S0022-0728(02)01100-2).
78. Meher SK, Rao GR. Ultralayered Co<sub>3</sub>O<sub>4</sub> for high-performance supercapacitor applications. *J Phys Chem C.* 2011;115(31):15646-15654.  
**DOI:**[10.1021/jp201200e](https://doi.org/10.1021/jp201200e).
79. Dong X, Xu H, Wang X, Huang Y, Chan-park MB, Zhang H. 3D Graphene-Cobalt Oxide Electrode for High-Performance Supercapacitor and Enzymeless Glucose Detection. *ACS Nano.* 2012;4(4):3206-3213.  
**DOI:**[10.1021/nn300097q](https://doi.org/10.1021/nn300097q).
80. Kumar R, Kim HJ, Park S, Srivastava A, Oh IK. Graphene-wrapped and cobalt oxide-intercalated hybrid for extremely durable super-capacitor with ultrahigh energy and power densities. *Carbon N Y.* 2014;79(1):192-202.  
**DOI:**[10.1016/j.carbon.2014.07.059](https://doi.org/10.1016/j.carbon.2014.07.059).
81. Yan J, Wei T, Qiao W, et al. Rapid microwave-assisted synthesis of graphene nanosheet/Co<sub>3</sub>O<sub>4</sub> composite for supercapacitors. *Electrochim Acta.* 2010;55(23):6973-6978.  
**DOI:**[10.1016/j.electacta.2010.06.081](https://doi.org/10.1016/j.electacta.2010.06.081).
82. Nguyen TT, Nguyen VH, Deivasigamani RK, Kharismadewi D, Iwai Y, Shim J-J. Facile synthesis of cobalt oxide/reduced graphene oxide composites for electrochemical capacitor and sensor applications. *Solid State Sci.* 2016;53:71-77.  
**DOI:**[10.1016/j.solidstatesciences.2016.01.006](https://doi.org/10.1016/j.solidstatesciences.2016.01.006).
83. Zhang M, Yan F, Tang X, et al. Flexible CoO-graphene-carbon nanofiber mats as binder-free anodes for lithium-ion batteries with superior rate capacity and cyclic stability. *J Mater Chem A.* 2014;2(16):5890-5897.  
**DOI:**[10.1039/C4TA00311J](https://doi.org/10.1039/C4TA00311J).
84. Deng W, Sun Y, Su Q, Xie E, Lan W. Porous CoO nanobundles composited with 3D graphene foams for supercapacitors electrodes. *Mater Lett.* 2014;137:124-127.  
**DOI:**[10.1016/j.matlet.2014.08.154](https://doi.org/10.1016/j.matlet.2014.08.154).
85. Deng W, Lan W, Sun Y, Su Q, Xie E. Porous CoO nanostructures grown on three-dimension graphene foams for supercapacitors electrodes. *Appl Surf Sci.* 2014;305:433-438.  
**DOI:**[10.1016/j.apsusc.2014.03.107](https://doi.org/10.1016/j.apsusc.2014.03.107).
86. Chen X, Chen K, Wang H, Xue D. Composition Design Upon Iron Element Toward Supercapacitor Electrode Materials. *Mater Focus.* 2015;4(1):78-80.  
**DOI:**[10.1166/mat.2015.1213](https://doi.org/10.1166/mat.2015.1213).
87. Nagarajan N, Zhitomirsky I. Cathodic electrosynthesis of iron oxide films for electrochemical supercapacitors. *J Appl Electrochem.* 2006;36(12):1399-1405.  
**DOI:**[10.1007/s10800-006-9232-x](https://doi.org/10.1007/s10800-006-9232-x).
88. Kim SI, Lee JS, Ahn HJ, Song HK, Jang JH. Facile route to an efficient NiO supercapacitor with a three-dimensional nanonetwork morphology. *ACS Appl Mater Interfaces.* 2013;5(5):1596-1603.  
**DOI:**[10.1021/am3021894](https://doi.org/10.1021/am3021894).
89. Reddy M V., Yu T, Sow CH, et al.  $\alpha$ -Fe<sub>2</sub>O<sub>3</sub> Nanoflakes as an Anode Material for Li-Ion Batteries. *Adv Funct Mater.* 2007;17(15):2792-2799.  
**DOI:**[10.1002/adfm.200601186](https://doi.org/10.1002/adfm.200601186).
90. Wang D, Wang Q, Wang T. Controlled synthesis of mesoporous hematite nanostructures and their application as electrochemical capacitor electrodes. *Nanotechnology.* 2011;22(13):135604.  
**DOI:**[10.1088/0957-4448/22/13/135604](https://doi.org/10.1088/0957-4448/22/13/135604).
91. Qu Q, Yang S, Feng X. 2D sandwich-like sheets of iron oxide grown on graphene as high energy anode material for supercapacitors. *Adv Mater.* 2011;23(46):5574-5580.  
**DOI:**[10.1002/adma.201103042](https://doi.org/10.1002/adma.201103042).
92. Zhang F, Zhang T, Yang X, et al. A high-performance supercapacitor-battery hybrid energy storage device based on graphene-enhanced electrode materials with ultrahigh energy density. *Energy Environ Sci.* 2013;6(5):1623-1632.  
**DOI:**[10.1039/c3ee40509e](https://doi.org/10.1039/c3ee40509e).
93. Ma Z, Huang X, Dou S, Wu J, Wang S. One-Pot Synthesis of Fe<sub>2</sub>O<sub>3</sub> Nanoparticles on Nitrogen-Doped Graphene as Advanced Supercapacitor Electrode Materials. *J Phys Chem C.* 2014;118(31):17231-17239.  
**DOI:**[10.1021/jp502226j](https://doi.org/10.1021/jp502226j).
94. Gholipour-Ranjbar H, Ganjali MR, Norouzi P, Naderi HR. Synthesis of cross-linked graphene aerogel/Fe<sub>2</sub>O<sub>3</sub> nanocomposite with enhanced supercapacitive performance. *Ceram Int.* 2016;42(10):12097-12104.  
**DOI:**[10.1016/j.ceramint.2016.04.140](https://doi.org/10.1016/j.ceramint.2016.04.140).
95. Khattak AM, Yin H, Ghazi ZA, et al. Three dimensional iron oxide/graphene aerogel hybrids as all-solid-state flexible supercapacitor electrodes. *RSC Adv.* 2016;6(64):58994-59000.  
**DOI:**[10.1039/C6RA11106H](https://doi.org/10.1039/C6RA11106H).
96. Song Z, Liu W, Wei W, et al. Preparation and electrochemical properties of Fe<sub>2</sub>O<sub>3</sub>/reduced graphene oxide aerogel (Fe<sub>2</sub>O<sub>3</sub>/rGOA) composites for supercapacitors. *J Alloys Compd.* 2016;685:355-363.  
**DOI:**[10.1016/j.jallcom.2016.05.323](https://doi.org/10.1016/j.jallcom.2016.05.323).
97. Srinivasan V, Weidner JW. Studies on the capacitance of nickel oxide films: effect of heating temperature and electrolyte concentration. *J Electrochem Soc.* 2000;147(3):880-885.  
**DOI:**[10.1149/1.1393286](https://doi.org/10.1149/1.1393286).
98. Zhao H, Pan L, Xing S, Luo J, Xu J. Vanadium oxides-reduced graphene oxide composite for lithium-ion batteries and supercapacitors with improved electrochemical performance. *J Power Sources.* 2013;222:21-31.  
**DOI:**[10.1016/j.jpowsour.2012.08.036](https://doi.org/10.1016/j.jpowsour.2012.08.036).
99. Saravanakumar B, Purushothaman KK, Muralidharan G. Interconnected V<sub>2</sub>O<sub>5</sub> Nanoporous Network for High-Performance Supercapacitors. *ACS Appl Mater Interfaces.* 2012;4(9):4484-4490.  
**DOI:**[10.1021/am301162p](https://doi.org/10.1021/am301162p).
100. Srinivasan V. An Electrochemical Route for Making Porous Nickel Oxide Electrochemical Capacitors. *J Electrochem Soc.* 1997;144(8):L210.  
**DOI:**[10.1149/1.1837859](https://doi.org/10.1149/1.1837859).
101. Nam K-W, Kim K-B. A Study of the Preparation of NiO<sub>x</sub> Electrode via Electrochemical Route for Supercapacitor Applications and Their Charge Storage Mechanism. *J Electrochem Soc.* 2002;149(3):A346.  
**DOI:**[10.1149/1.1449951](https://doi.org/10.1149/1.1449951).
102. Zhao B, Wang T, Jiang L, et al. NiO mesoporous nanowalls grown on RGO coated nickel foam as high performance electrodes for supercapacitors and biosensors. *Electrochim Acta.* 2016;192:205-215.  
**DOI:**[10.1016/j.electacta.2016.01.211](https://doi.org/10.1016/j.electacta.2016.01.211).
103. Jing M, Wang C, Hou H, et al. Ultrafine nickel oxide quantum dots embedded with few-layer exfoliative graphene for an asymmetric supercapacitor: Enhanced capacitances by alternating voltage. *J Power Sources.* 2015;298:241-248.  
**DOI:**[10.1016/j.jpowsour.2015.08.039](https://doi.org/10.1016/j.jpowsour.2015.08.039).
104. Trung NB, Tam T V, Dang DK, et al. Facile synthesis of three-dimensional graphene/nickel oxide nanoparticles composites for high performance supercapacitor electrodes. *Chem Eng J.* 2015;264:603-609.  
**DOI:**[10.1016/j.cej.2014.11.140](https://doi.org/10.1016/j.cej.2014.11.140).
105. Banerjee PC, Lobo DE, Middag R, Ng WK, Shaibani ME, Majumder M. Electrochemical Capacitance of Ni-Doped Metal Organic Framework and Reduced Graphene Oxide Composites:

- More than the Sum of Its Parts. *ACS Appl Mater Interfaces*. 2015;7(6):3655-3664.  
DOI:10.1021/am508119c.
106. Zhao H, Pan L, Xing S, Luo J, Xu J. Vanadium oxides e reduced graphene oxide composite for lithium-ion batteries and supercapacitors with improved electrochemical performance. *J Power Sources*. 2013;222:21-31.  
DOI:10.1016/j.jpowsour.2012.08.036.
107. Lee M, Balasingam SK, Jeong HY, et al. One-step hydrothermal synthesis of graphene decorated V<sub>2</sub>O<sub>5</sub> nanobelts for enhanced electrochemical energy storage. *Sci Rep*. 2015;5:8151.  
DOI:10.1038/srep08151.
108. Yilmaz G, Lu X, Ho GW. Cross-linker mediated formation of sulfur-functionalized V<sub>2</sub>O<sub>5</sub>/graphene aerogels and their enhanced pseudocapacitive performance. *Nanoscale*. 2017:802-811.  
DOI:10.1039/C6NR08233E.
109. Hu X, Yan Z, Li Q, et al. Graphene/vanadium oxide hybrid electrodes for electrochemical capacitor. *Colloids Surfaces A Physicochem Eng Asp*. 2014;461(1):105-112.  
DOI:10.1016/j.colsurfa.2014.07.032.
110. Zhao H, Pan L, Xing S, Luo J, Xu J. Vanadium oxides reduced graphene oxide composite for lithium-ion batteries and supercapacitors with improved electrochemical performance. *J Power Sources*. 2013;222(July 2015):21-31.  
DOI:10.1016/j.jpowsour.2012.08.036.
111. Choudhury A, Bonso JS, Wunch M, Yang KS, Ferraris JP, Yang DJ. In-situ synthesis of vanadium pentoxide nanofibre/exfoliated graphene nanohybrid and its supercapacitor applications. *J Power Sources*. 2015;287:283-290.  
DOI:10.1016/j.jpowsour.2015.04.062.
112. Liu T, Pell WG, Conway BE. Self-discharge and potential recovery phenomena at thermally and electrochemically prepared RuO<sub>2</sub> supercapacitor electrodes. *Electrochim Acta*. 1997;42(23-24):3541-3552.  
DOI:10.1016/S0013-4686(97)81190-5.
113. Wang W, Guo S, Lee I, et al. Hydrous Ruthenium Oxide Nanoparticles Anchored to Graphene and Carbon Nanotube Hybrid Foam for Supercapacitors. *Sci Rep*. 2015;4(1):4452.  
DOI:10.1038/srep04452.
114. Yang F, Zhang L, Zuzuarregui A, et al. Functionalization of Defect Sites in Graphene with RuO<sub>2</sub> for High Capacitive Performance. *ACS Appl Mater Interfaces*. 2015;7(37):20513-20519.  
DOI:10.1021/acsami.5b04704.
115. Yang Y, Liang Y, Zhang Y, et al. Three-dimensional graphene hydrogel supported ultrafine RuO<sub>2</sub> nanoparticles for supercapacitor electrodes. *New J Chem*. 2015;39(5):4035-4040.  
DOI:10.1039/C5NJ00062A.
116. Hwang JY, El-Kady MF, Wang Y, et al. Direct preparation and processing of graphene/RuO<sub>2</sub> nanocomposite electrodes for high-performance capacitive energy storage. *Nano Energy*. 2015; 18:57-70.  
DOI:10.1016/j.nanoen.2015.09.009.
117. Hu C-C, Wang C-W, Chang K-H, Chen M-G. Anodic composite deposition of RuO<sub>2</sub>/reduced graphene oxide/carbon nanotube for advanced supercapacitors. *Nanotechnology*. 2015;26(27):274004.  
DOI:10.1088/0957-4484/26/27/274004.
118. Li F, Song J, Yang H, et al. One-step synthesis of graphene/SnO<sub>2</sub> nanocomposites and its application in electrochemical supercapacitors. *Nanotechnology*. 2009;20(45):455602.  
DOI:10.1088/0957-4484/20/45/455602.
119. Liu R, Ma L, Niu G, et al. Oxygen-Deficient Bismuth Oxide/Graphene of Ultrahigh Capacitance as Advanced Flexible Anode for Asymmetric Supercapacitors. *Adv Funct Mater*. 2017;3(July):7-8.  
DOI:10.1002/adfm.201701635.
120. Liu D-Q, Yu S-H, Son S-W, Joo S-K. Electrochemical Performance of Iridium Oxide Thin Film for Supercapacitor Prepared by Radio Frequency Magnetron Sputtering Method. *ECS Trans*. 2008;16(1):103-109.  
DOI:10.1149/1.2985632.
121. Wang Y, Guo CX, Liu J, Chen T, Yang H, Li CM. CeO<sub>2</sub> nanoparticles/graphene nanocomposite-based high performance supercapacitor. *Dalton Trans*. 2011;40(24):6388-6391.  
DOI:10.1039/c1dt10397k.
122. Mendoza-Sánchez B, Brousse T, Ramirez-Castro C, Nicolosi V, S. Grant P. An investigation of nanostructured thin film α-MoO<sub>3</sub> based supercapacitor electrodes in an aqueous electrolyte. *Electrochim Acta*. 2013;91:253-260.  
DOI:10.1016/j.electacta.2012.11.127.
123. Dong X, Shen W, Gu J, et al. MnO<sub>2</sub>-embedded-in-mesoporous-carbon-wall structure for use as electrochemical capacitors. *J Phys Chem B*. 2006;110(12):6015-6019.  
DOI:10.1021/jp056754n.
124. He G, Li J, Chen H, et al. Hydrothermal Preparation of Co<sub>3</sub>O<sub>4</sub>@graphene Nanocomposite for Supercapacitor with Enhanced Capacitive Performance. Vol 82.; 2012.  
DOI:10.1016/j.matlet.2012.05.048.
125. Peng L, Peng X, Liu B, Wu C, Xie Y, Yu G. Ultrathin Two-Dimensional MnO<sub>2</sub>/Graphene Hybrid Nanostructures for High-Performance, Flexible Planar Supercapacitors. *Nano Lett*. 2013;13(5):2151-2157.  
DOI:10.1021/nl400600x.
126. Moussa M, Shi G, Wu H, et al. Development of flexible supercapacitors using an inexpensive graphene/PEDOT/MnO<sub>2</sub> sponge composite. *Mater Des*. 2017;125:1-10.  
DOI:10.1016/j.matdes.2017.03.075.
127. Jia HN, Lin JH, Liu YL, et al. Nanosized core-shell structured graphene-MnO<sub>2</sub> nanosheet arrays as stable electrodes for superior supercapacitors. *J Mater Chem A*. 2017;5(21):10678-10686.  
DOI:10.1039/C7TA02627G.
128. Zhao K, Lyu K, Liu S, Gan Q, He Z, Zhou Z. Ordered porous Mn<sub>3</sub>O<sub>4</sub>@N-doped carbon/graphene hybrids derived from metal-organic frameworks for supercapacitor electrodes. *J Mater Sci*. 2017;52(1):446-457.  
DOI:10.1007/s10853-016-0344-3.
129. Yang YY, Hu ZA, Zhang ZY, et al. Reduced graphene oxide-nickel oxide composites with high electrochemical capacitive performance. *Mater Chem Phys*. 2012;133(1):363-368.  
DOI:10.1016/j.matchemphys.2012.01.039.
130. Karthik R, Thambidurai S. Synthesis of RGO-Co doped ZnO/PANI hybrid composite for supercapacitor application. *J Mater Sci Mater Electron*. 2017;28(13):9836-9851.  
DOI:10.1007/s10854-017-6738-4.
131. Li J, Sun Y, Li D, Yang H, Zhang X, Lin B. Novel ternary composites reduced-graphene oxide/zinc oxide/poly(p-phenylenediamine) for supercapacitor: Synthesis and properties. *J Alloys Compd*. 2017;708:787-795.  
DOI:10.1016/j.jallcom.2017.03.062.
132. Ren X, Guo C, Xu L, Li T, Hou L, Wei Y. Facile synthesis of hierarchical mesoporous honeycomb-like NiO for aqueous asymmetric supercapacitors. *ACS Appl Mater Interfaces*. 2015;7(36):19930-19940.  
DOI:10.1021/acsami.5b04094